The Thesis Committee for Gregory Fred Dellinger
Certifies that this is the approved version of the following thesis:

The Use of Time Domain Reflectometry Probes for the Moisture Monitoring of a Drilled Shaft Retaining Wall in Expansive Clay

APPROVED BY
SUPERVISING COMMITTEE:

Supervisor:

Robert B. Gilbert

Jorge G. Zornberg

The Use of Time Domain Reflectometry Probes for the Moisture Monitoring of a Drilled Shaft Retaining Wall in Expansive Clay

by

Gregory Fred Dellinger, B.S.

Thesis

Presented to the Faculty of the Graduate School of

The University of Texas at Austin

in Partial Fulfillment

of the Requirements

for the Degree of

Master of Science in Engineering

The University of Texas at Austin

August 2011

Dedication

To everyone who reads this.

Acknowledgements

I would like to thank my advisor, Dr. Robert B. Gilbert, for his support and guidance. Also, I would like to thank Dr. Jorge G. Zornberg for taking the time to review this and his assistance and I would like to thank Dr. Chadi El Mohtar for his assistance. I would like to thank Andrew Brown and Trent Ellis for their invaluable work and contributions to this project. The support and encouragement of my family is also greatly appreciated.

I would also like to extend my gratitude and thank Fugro Consultants, Inc. for their financial support.

Abstract

The Use of Time Domain Reflectometry Probes for the Moisture Monitoring of a Drilled Shaft Retaining Wall in Expansive Clay

Gregory Fred Dellinger, M.S.E.

The University of Texas at Austin, 2011

Supervisor: Robert B. Gilbert

Currently there is no consensus on how to account for the lateral earth pressures when designing drilled shaft retaining walls in expansive clay soils. Typically an equivalent fluid pressure is assumed which can range from 40 psf/ft to over 100 psf/ft. The range of assumptions currently in use can cause more than a factor of two difference in the maximum bending moment in the shaft. This range could cause the walls to be over-designed or under-designed.

A full-scale test drilled shaft retaining wall was constructed on a site underlain by approximately 50 feet of the expansive Taylor Clay. Analysis of the wall is intended to provide information to be considered in design about the effects of the moisture cycles which cause shrinking and swelling.

In order to monitor the moisture changes within the clay, 20 Time Domain Reflectometry (TDR) probes were installed behind the wall. This thesis discusses the monitoring plan, calibration, installation, and initial results from these probes. The objectives of this thesis is to provide information regarding the site conditions and

reasons for using TDR probes for this project and to describe the monitoring plan, calibration, installation, and the field performance of the TDR probes and the moisture values that have been seen on the site to date.

Previous studies show that difficulties can be expected when using TDR probes in highly plastic clays. Results from this study are typical of these results seen previously. The initial results show that 4 of the 20 probes are recording reasonable waveforms. However, the waveforms cannot be analyzed using conventional methods. This result was because the waveform reflection that indicates the end of the probe cannot be defined due to attenuation of the signal, which is typical of highly conductive soils. Also, the large amount of scatter in the electrical conductivity values does not allow for the moisture content to be correlated to the electrical conductivity.

In order to use the TDR probes to measure moisture content at the project site, an alternative method needs to be employed to analyze available waveforms. If another method can be successfully employed for the functional probes, the subsequent step would involve recovering the probes that are not functioning properly in order to get a moisture profile along the full cantilevered height of the wall. Direct moisture measurements should also be taken periodically to provide a moisture profile.

Table of Contents

List of Tables

List of Figures

CHAPTER 1: INTRODUCTION

1.1: Motivation

Expansive clay soils are common throughout Texas and the United States. These expansive soils have been reported to cause billions of dollars in structural damage a year in the United States (Jones and Holtz, 1973). In Texas, retaining walls are often used in areas with expansive clay soils. An understanding of the behavior of the interaction between expansive clay and retaining walls is important in being able to design and construct these walls properly and cost efficiently.

Drilled shaft retaining walls are commonly used throughout Texas, especially by the Texas Department of Transportation (TxDOT). Recently in the state of Texas, there have been questions regarding the performance of these drilled shaft walls in the expansive clay soils.

When expansive clay soils experience moisture changes, the clay will shrink and swell. When estimating the lateral earth pressures acting on a wall, and important challenge is to predict swell pressures from moisture changes. The uncertainties that are associated with designing a drilled shaft retaining wall in expansive clay are what the distributions of lateral earth pressures versus depth below the ground surface should be and how the moisture cycles of the clay should be considered. It is currently not clear how to account for the shrinking and swelling of the expansive clay soils and the earth pressures applied on a wall during these processes. It is common practice to assume an equivalent fluid pressure for design. Typical fluid pressures used range from 40 to 80 psf/ft with some engineers using more than 100 psf/ft. A range of 55 to 80 psf/ft is recommended for expansive clay soils by the Foundations Engineering Handbook (1991).

The range of assumptions currently in practice can cause more than a factor of two difference in the maximum bending moment in the shaft (Brown et al., 2011). This uncertainty could cause walls to be over-designed or under-designed, depending on the assumptions made.

1.2: TxDOT Research Project

While TxDOT has not seen widespread failures of their drilled shaft retaining walls in expansive clay, they would benefit from a better understanding of the pressures that can realistically be exerted on drilled shaft walls. TxDOT has provided funding to the University of Texas at Austin in order to determine the performance of their current drilled shaft retaining walls in expansive clays and to provide guidance in the design of these walls by instrumenting and monitoring a full-scale test wall. The goal of the test wall is to assess the effects of seasonal moisture changes on the lateral earth pressures acting on the wall and use the information to provide TxDOT guidelines for the design of drilled shaft retaining walls in expansive clay soils.

The TxDOT 0-6603 research project involves instrumenting and monitoring a full-scale drilled shaft retaining wall constructed in the expansive Taylor Clay. This retaining wall is to be monitored for three years after construction. The wall has been instrumented with optical strain gauges to measure the bending strains within the shafts as they deflect and inclinometers are installed to measure the deflected shape of the wall over time. Thermocouples within the instrumented shafts are used to measure the temperature within the concrete. A linear potentiometer is connected to the wall to compare the deflection at ground level with the inclinometer data. Time Domain Reflectometry (TDR) probes are installed in the soil behind the wall to measure moisture

fluctuations. A rain gauge on site is used to measure the amount of rainfall in the area of the wall. Also, a piezometer is located near the wall to measure the location of the water table. Currently the wall has been monitored for approximately 16 months.

1.3: Objectives for Thesis

This thesis deals with aspects of the initial construction and monitoring of the drilled shaft retaining wall. This study includes the calibration, installation, and initial performance of the TDR probes. The objectives of this thesis are the following:

1. Present background regarding TDR probes
2. Describe the site conditions and reason for using TDR probes
3. Discuss the monitoring plan to measure the moisture on the site
4. Describe the calibration and installation procedure
5. Discuss the field performance
6. Present the conclusions and recommendations for further study

1.4: Organization of Thesis

This thesis is divided into seven chapters. Chapter 1 consists of the introduction material and is followed by the background of previous research in Chapter 2. The background includes reviews of Taylor Clay, TDR probes and their use in expansive clay soils. Chapter 3 discusses the site conditions and test wall for the TxDOT 0-6603 project. The moisture monitoring plan and calibration are discussed in Chapter 4. Chapter 5 discusses the installation of the TDR probes into the soil. The field performance of the

probes and a discussion of the results are provided in Chapter 6. Chapter 7 presents a short summary of the findings and the conclusions drawn from this study.

CHAPTER 2: BACKGROUND

The background gathered from past studies is presented in this chapter. Specifically, how Time Domain Reflectometry (TDR) probes work, and previous studies using TDR probes.

2.1: Theory for Time Domain Reflectometry (TDR) Probes

Originally, TDR technology was developed for to find small breaks in transmission lines (Antle, 1997, Siddiqui et al., 2000). The technology was adapted into a method for determining the dielectric constant of soil. Water has a high dielectric constant compared to the soil solids or air, which makes the soil dielectric constant highly dependent upon the volume of water in the soil (Siddiqui et al., 2000). An empirical relationship between volumetric water content and the dielectric constant of the soil was discovered by Topp et al. (1980).

A TDR system works by sending an electromagnetic waveform through the system to the TDR probes. The dielectric constant of the soil causes a change in the velocity of the waveform that is reflected and recorded. By using the reflected waveform, the dielectric constant can be estimated. The volumetric water content can then be estimated by using the empirical relationship such as that established by Topp et al. (1980).

A sample TDR probe used for this study is shown in Figure 2.1. The probes can vary in size, metal rod spacing and lengths. The electromagnetic pulse is sent through the center rod and the outer two rods act as a shield. These probe designs make it so an average volumetric water content is being measured of a small volume of soil. The time for the reflected waveform is measured during a period of time of nanoseconds.

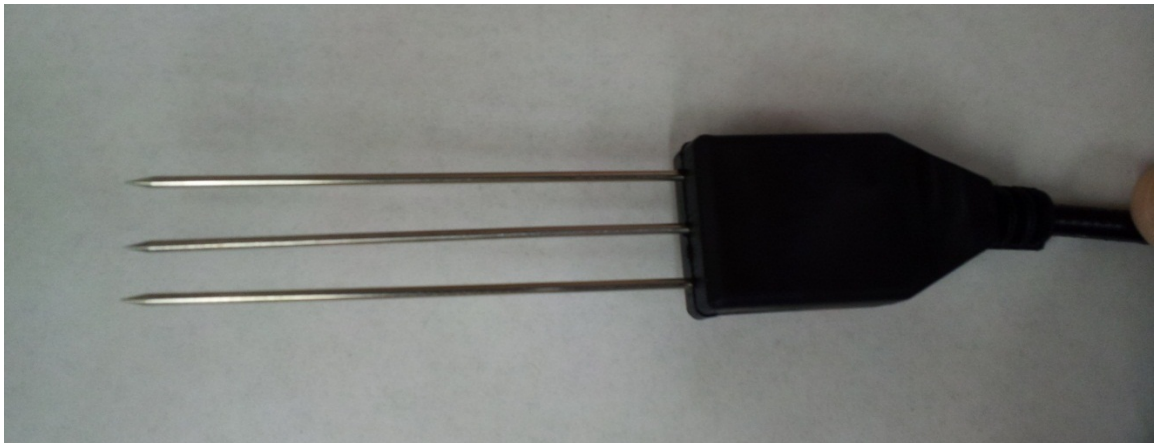

Figure 2.1: A sample TDR probe used in this study (rod length: 7.5 cm; rod diameter: 0.159 cm)

The reflected waveform that is measured consists of three reflection points. These points are shown as points 1-3 in Figure 2.2. Point 1 is the reflection point between the cable and the probe rods that are surrounded by the probe head. This portion of the probe is still not in contact with the soil. The second reflection point (point 2) is the transition point from the rods surrounded by the probe head and the rods in contact with the soil. The third reflection point (point 3) is the point where the signal reaches the end of the metal rod. Using the distance between the second and third point, the dielectric constant of the soil can be estimated.

Figure 2.2 shows a typical waveform taken from a TDR probe (Campbell Scientific, Inc., 2010). The y-axis consist of reflection coefficient and the x-axis can be presented as time, distance, or waveform data point; depending on the preference of the operator and the method used to analyze the waveform. The data points recorded to generate the waveform are taken on the order of nanoseconds.

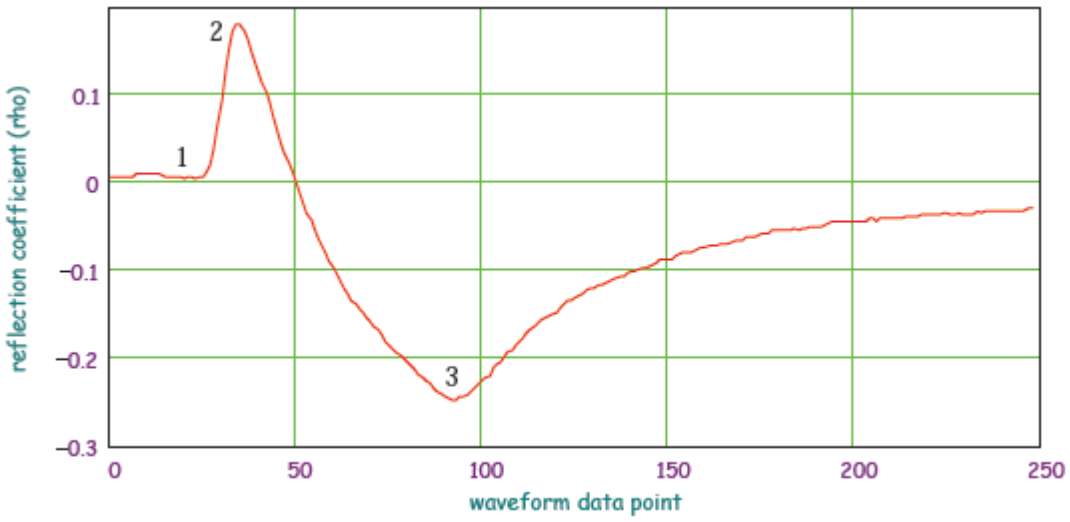

Figure 2.2: A typical waveform showing the key points (Campbell Scientific, Inc., 2010)

Siddiqui et al. (2000) described the relationship between the dielectric constant and the time between points 2 and 3. The velocity (v) of the electromagnetic wave through the probe is equal to the distance travelled (2L) divided by the time between points 2 and 3 (Equation 2.1), where 2L is twice the length of the probe and t is the time between points 2 and 3.

$$v = \frac{2L}{t} \qquad \text{(Equation 2.1)}$$

Siddiqui et al. (2000) also shows the velocity of the electromagnetic wave is equal to the speed of light through a vacuum (c) divided by the square root of the apparent dielectric constant of the soil (K_a).

$$v = \frac{c}{\sqrt{K_a}} \qquad \text{(Equation 2.2)}$$

The combination of Equation 2.1 and Equation 2.2 results in Equation 2.3 to determine the apparent dielectric constant for the soil (Siddiqui et al., 2000). Only the time between points 2 and 3 is needed to determine the apparent dielectric constant of the soil as the speed of light and the length of the probes are constants.

$$K_a = \left(\frac{ct}{2L}\right)^2 \qquad \text{(Equation 2.3)}$$

Campbell Scientific, Inc. uses an algorithm in their programming that determines the electrical apparent dielectric constant by using an apparent probe length (L_a) between point 2 and point 3. When determining the dielectric constant using lengths, the apparent length is the length that the probe appears to be when viewing the waveform. The theory of the algorithm is the same as presented by Siddiqui et al. (2000), but it uses an apparent probe length that is equal to the speed of light in a vacuum multiplied by the time and divided by 2 (Campbell Scientific, Inc., 2010).

$$t = \frac{2L\sqrt{K_a}}{c} \qquad \text{(Equation 2.4)}$$

Combining Equation 2.4 and Equation 2.3 produces the equation used by Campbell Scientific, Inc. in their algorithm (Campbell Scientific, Inc., 2010).

$$\frac{L_a}{L} = \sqrt{K_a} \qquad \text{(Equation 2.5)}$$

With the apparent dielectric constant, an empirical relationship developed by Topp et al. (1980) can be used to estimate the volumetric water content of the soil (θ_v) (Equation 2.6).

$$\theta_v = 5.3 * 10^{-2} + 2.92 * 10^{-2} K_a - 5.5 * 10^{-4} {K_a}^2 + 4.3 * 10^{-6} {K_a}^3 \qquad \text{(Equation 2.6)}$$

The TDR probes also record the bulk electrical conductivity of the soil (σ). This is done by measuring the reflection coefficient (ρ). The reflection coefficient ranges between plus and minus one and is the ratio of the reflected voltage to the applied voltage (Campbell Scientific, Inc., 2010). Equation 2.7 is used to calculate the bulk electrical conductivity using the reflection coefficient (Giese and Tiemann, 1975).

$$\sigma = \frac{K_p}{Z_c} \frac{1-\rho}{1+\rho} \qquad \text{(Equation 2.7)}$$

where K_p is a probe constant determined by a calibration and Z_c is the cable impedance. The probe constant is determined by doing a calibration and is the ratio of the electrical conductivity to the electrical conductance.

2.2: Studies Using TDR Probes

Topp et al. (1980) introduced an empirical method of using TDR probes to determine water content of soil. A wide range of soil specimens, from sandy loam to clay, were used to establish the empirical equation (Equation 2.6). Topp et al. (1980) concluded that electrical losses from the TDR system were negligible, the dielectric constant is not frequency dependent from the range of 1 MHz to 1 GHz, there was no

significant temperature dependence, and the equation was almost independent of soil density, texture, and salt content. However, the specific surface area of the soil particles is important when correlating the dielectric constant of the soil to the moisture content. Lower moisture contents have a lower dielectric constant that is closer to what would typically be for water in ice structures, and higher moisture contents had higher dielectric constant values.

Empirical relationships for determining the volumetric water content from TDR probe measurements have been reported to be inaccurate for high plasticity clays (Reedy and Scanlon, 2002, and Kuhn, 2005). Kuhn (2005) noticed a significant difference between the volumetric water content obtained using the Topp et al. (1980) equation and the actual value in the Eagle Ford Clay. The Eagle Ford formation used had a Plasticity Index of 49 percent. Both the Eagle Ford Clay and the Taylor Clay used for this study are highly plastic clays that can be found in the Austin area. Kuhn (2005) conducted laboratory experiments using the TDR probes to compare the volumetric water content at a measured dielectric constant compared to the results of using the Topp et al. (1980) equation. Figure 2.3 shows the results where the volumetric water content is plotted versus the square root of the dielectric constant.

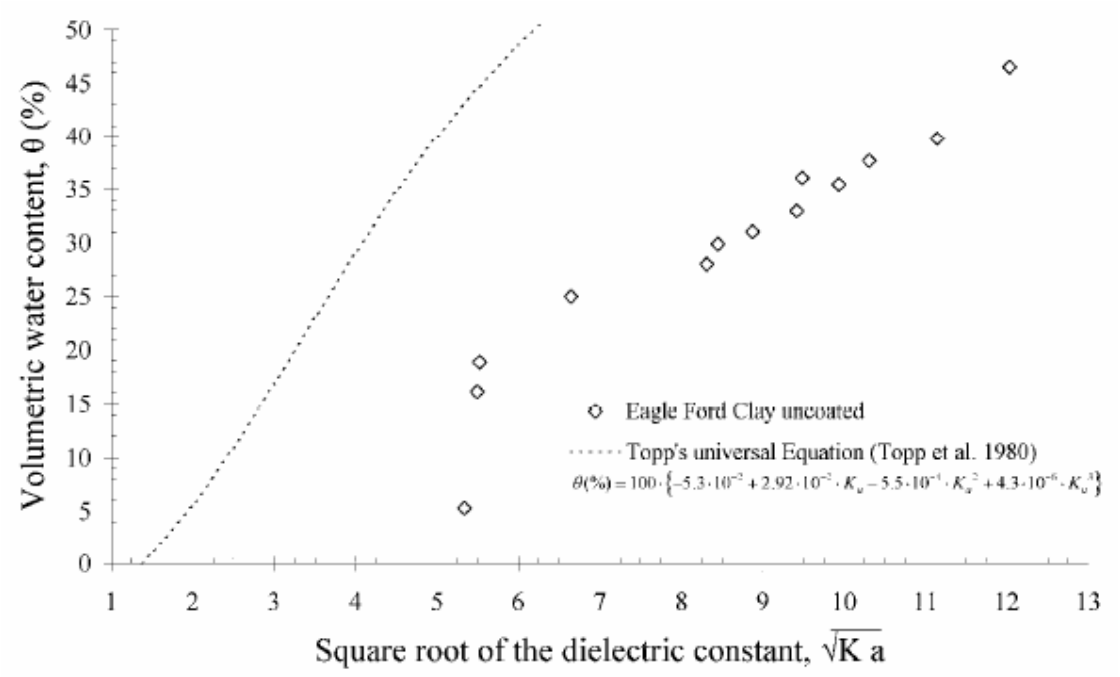

Figure 2.3: Comparison of the Topp et al. (1980) equation and the actual volumetric water content in Eagle Ford Clay (Kuhn 2005)

When TDR probes are used in highly plastic clays, the waveforms often show poor signal reflections. This result is due to the high electrical conductivity of the highly plastic clays, which cause attenuation of the signal (Jones and Or, 2004). Typically when the electrical conductivity increases, the water content is overestimated (Campbell Scientific, Inc., 2010). Several studies have reported results that show a reflected waveform that does not show the reflection that defines the end of the probe (Point 3 in Figure 2.2) (Reedy and Scanlon, 2002, Chen et al., 2007, Jones and Or, 2004).

In order to use TDR probes in highly conductive soils, different methods have been utilized. Kuhn (2005) and Moret-Fernandez et al. (2009) used coating on the probes to help reduce the interference of the electrical conductivity of the soil. Moret-Fernandez et al. (2009) used probes partially coated with a different percentage of the probe being

covered. It was noticed that almost completely coated the probe allowed for the inflection that indicates the end of the probe to be seen in the waveform. An issue with the coating is that the coating has the potential to wear over time which would affect the calibration of the probe.

Chen et al. (2007) developed a model-based method that analyzes the reflection of the waveform at the surface of the soil instead of at the end of the probes to determine the dielectric constant. The approach showed a reasonable accuracy in estimating the dielectric constant of the soil. To use the procedure a calibration needs to be performed first.

Jones and Or (2004) presented a method to transform the waveform data so it could be analyzed in the frequency domain. An artificially generated step function in the time domain is used to provide the necessary input signal. Smaller probes (on the order of 2 cm) are needed for this analysis in the frequency domain in order to reduce the signal attenuation compared to the optimal 10 to 15 cm probe lengths for conventional time domain methods. This method also needs a precise calibration in order to work properly.

The benefits of using a TDR system instead of the FDR system were reported to be less affected by soil type and temperature (Seyfried and Murdock, 2004). TDR probes perform well in soils with higher electrical conductivities as long as they are below a limit of 5.0 dS/m, according to the TDR100 Manual (Campbell Scientific, Inc., 2010). Based on their studies, Seyfried and Murdock (2004) expect that the FDR probes used in their studies would be more sensitive to soil conditions than the TDR probes used. The TDR system also does not typically need to have a soil specific calibration performed to produce reliable results.

2.2.1: TDR ROD ALIGNMENT

Campbell Scientific Inc. performed a test in air and water to determine the effects of the TDR rods not being in the correct alignment (Brown 2011). CS 640 probes, which have a 7.5 centimeter probe length, were used with 20 feet of cable. Tests were performed with the rod alignment being correct and with three different rod alignment scenarios. The first two scenarios consisted of deflecting the outside rods outward and inward four millimeters. In the third scenario, the center rod was deflected out of alignment by four millimeters and the outer rods were deflected outward four millimeters. The tests show that the measured results were not affected by more than 0.03 percent. Campbell Scientific Inc. also noted that the results may not be typical when applied to soils due to the problem of causing compaction of the soil or causing air voids to be developed.

CHAPTER 3: SITE CONDITIONS AND TEST WALL

The drilled shaft retaining test wall is explained in this chapter. Specifically, the design of the wall and the instrumentation within the wall and on site are described. Also, the site location and conditions are discussed. A picture of the retaining wall is shown in Figure 3.1. The pouring of the concrete shafts was done from March 30, 2010 to April 6, 2010. Excavation was gradually done during the month of August 2010 and the shotcrete facing was added on the wall on October 1, 2010.

Figure 3.1: A view of the test wall after excavation and installation of the shotcrete facing

3.1: Site Conditions

The project site is located in Manor, TX underlained by approximately 50 feet of the highly expansive Taylor Clay. The clay is blocky, highly fissured and heavily overconsolidated. A picture of a sample taken from the Taylor Clay on site is shown in Figure 3.2.

Figure 3.2: A sample of the Taylor Clay at the project site

On January 12 and 13, 2010, three borings were drilled to a depth of 50 feet by Fugro Consultants, Inc. During the borings, Texas Cone Penetration (TCP) tests and Standard Penetration Tests (SPT) were performed and split-spoon samples were taken in order to provide information consistent with the standard of practice in Texas. An inclinometer and a piezometer were installed in two of the borings. The third boring was backfilled with cuttings.

3.1.1: MOISTURE CONTENTS AND ATTERBERG LIMITS

Atterberg Limits were performed according to the standard of practice. Liquid Limits reached ranged from approximately 50 percent to over 100 percent over the length of the profile. The Liquid Limits measured below approximately 5 feet were all above 80 percent. Plastic Limits were between approximately 20 and 30 percent. The water contents on January 12, 2010 were between 20 and 40 percent. Figure 3.3 shows the Atterberg Limits and the moisture contents from January 12, 2010.

3.1.2: UNDRAINED SHEAR STRENGTHS

Several Unconsolidated Undrained (UU) triaxial tests were performed on the split-spoon samples taken from the field investigation. Two tests were done by trimming the samples to a 1.5 inch diameter. Due to the highly fissured nature of the clay, the trimming process was difficult. The remaining tests were done at the Fugro laboratory in Austin, Texas, using test specimens with the split-spoon diameter of 2.7 inches. The strengths ranged from 1500 psf to over 6000 psf. The undrained strength profile is shown in Figure 3.4.

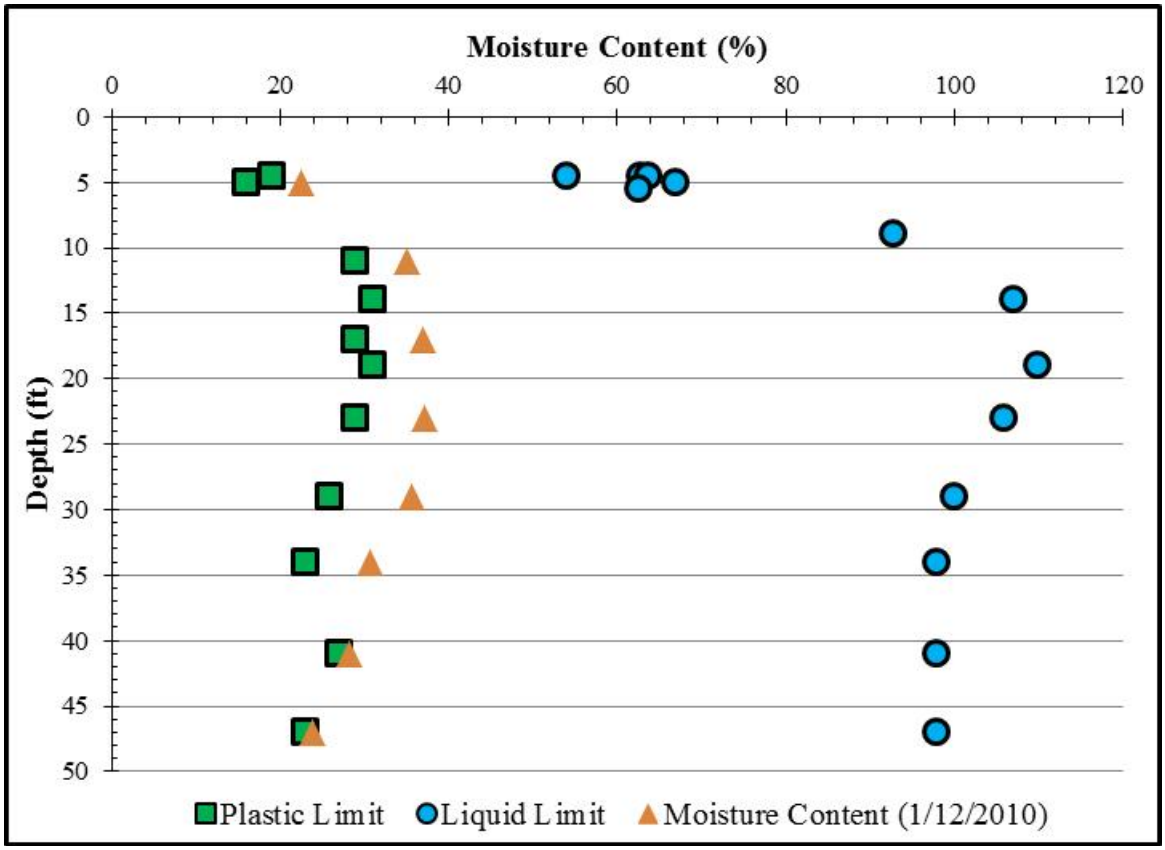

Figure 3.3: The Atterberg Limits of the Taylor Clay and the water content on January 12, 2010

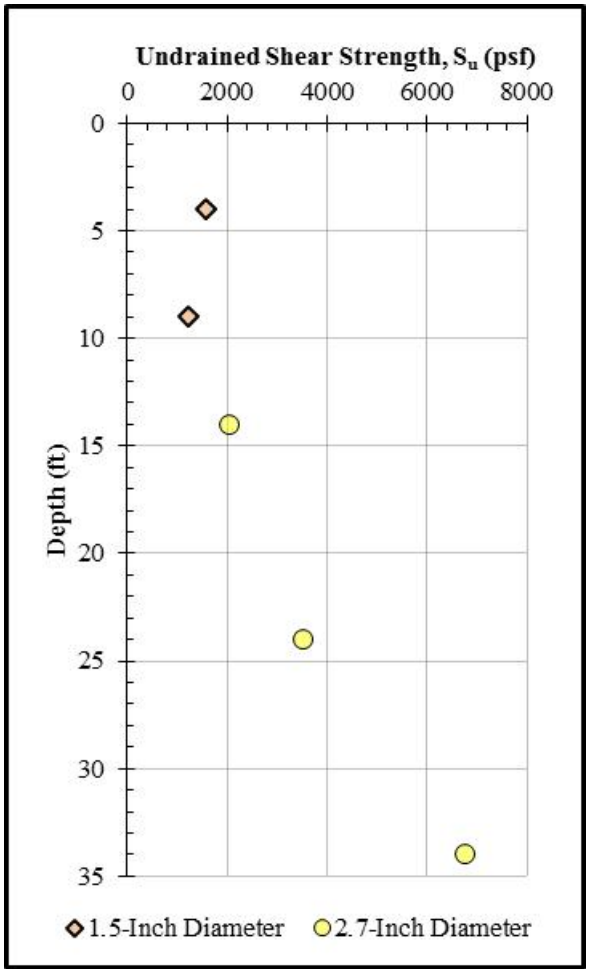

Figure 3.4: Undrained shear strength profile from UU testing

3.2: Test Wall

The test wall was designed to be in accordance with typical TxDOT design procedures, but flexible enough to see movements from the wall in order to estimate the earth pressures exerted on the wall. This wall consists of 25 drilled shafts with a 24 inch diameter spaced six inches edge to edge (Figure 3.5). The shafts are embedded to depths from 18 to 35 feet below the ground surface with the deepest shafts being in the center

(Figure 3.6). At the center of the wall, the cantilever height is 15 feet, the penetration depth is 20 feet, and top of the shafts is four feet above the ground surface (Figure 3.7). The four foot stickup allows for the possibility of doing a lateral load test at the end of the project. The rebar reinforcing cage contains 12 #7 bars.

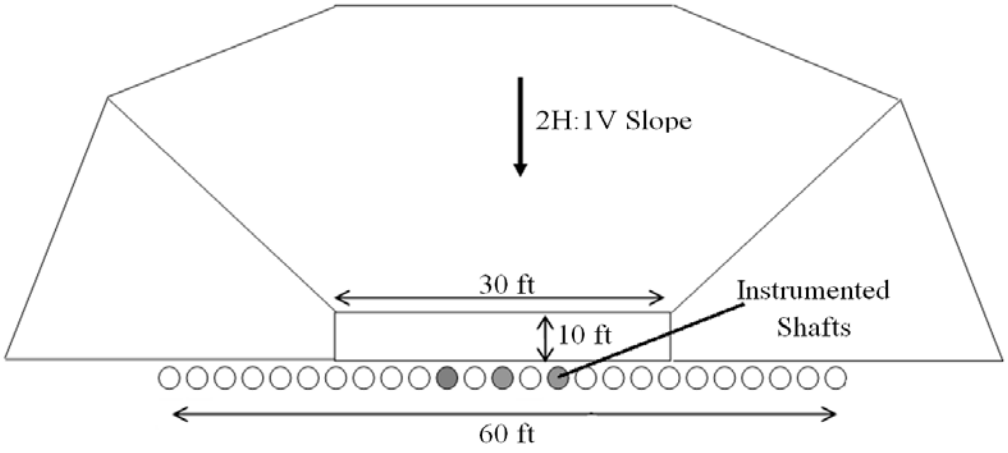

Figure 3.5: Plan view of the wall and excavation

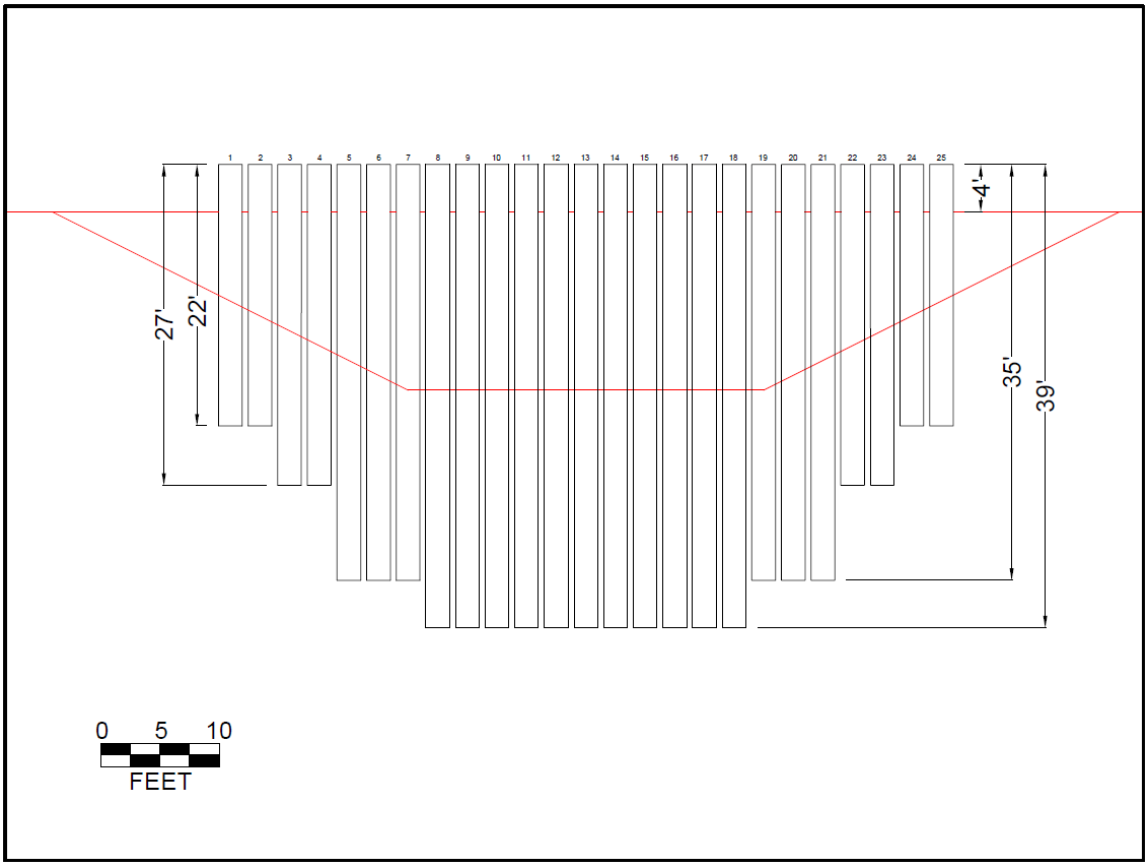

Figure 3.6: Layout of the drilled shafts

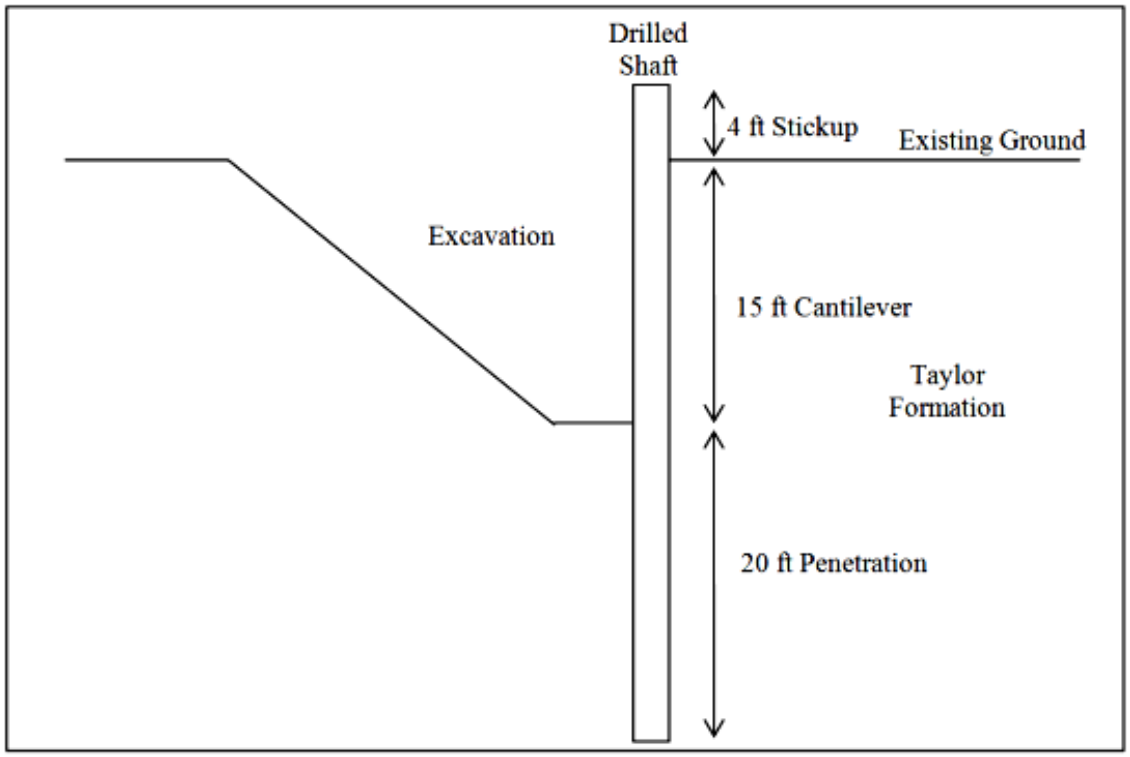

Figure 3.7: Cross-section of wall and excavation

3.2.1: INSTRUMENTATION FOR DISPLACEMENT AND STRESS

There are three shafts instrumented for this project (Figure 3.5). Within each instrumented shaft is an inclinometer casing and 30 optical strain gauges; 15 on the tension side and 15 on the compression side, spaced two feet center to center. The optical strain gauge wires are protected in a slotted PVC pipe. One inclinometer is also installed 5.5 feet behind the wall. There are three thermocouples within the center shaft at depths of three, 15, and 29 feet below the ground surface and seven thermocouples in a non-instrumented shaft spaced every two feet from depths of one to 13 feet below the ground surface. Figure 3.8 shows an instrumented shaft placed in the ground before concrete

placement. Additionally, there is a linear potentiometer attached to the top of one of the shafts to measure the lateral deformation of the wall at the ground surface.

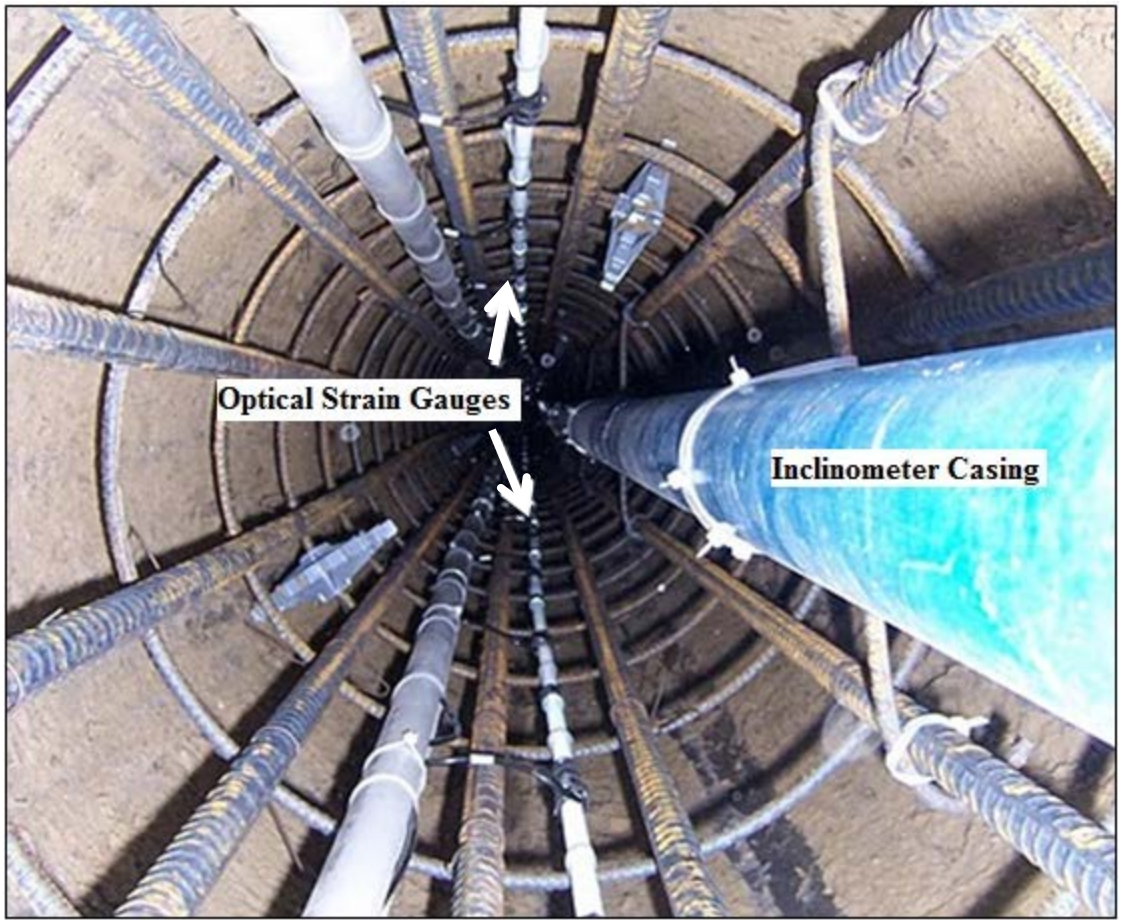

Figure 3.8: Instrumented cage before concrete placement

CHAPTER 4: MOISTURE MONITORING PLAN AND CALIBRATION

The description of the moisture monitoring plan and the system schematic of the moisture monitoring plan are presented in this chapter. Also, the description of the calibration performed on the TDR system is presented.

4.1: Moisture Monitoring Plan

TDR probes were used to monitor the volumetric water content of the soil on site. The system consists of 20 Campbell Scientific, Inc. CS645-L probes with 70 feet of LMR-200 low loss cable length, a Campbell Scientific, Inc. TDR100, three Campbell Scientific, Inc. SDX50 multiplexers, and a Campbell Scientific, Inc. CR1000. The TDR100 generates the signals that are sent to the probes and the CR1000 logs the data. CS645-L probes are manufactured with rod lengths of 7.5 centimeters (2.95 inches) and rod diameters of 0.159 centimeters (0.06 inches).

The TDR probes were to be installed at various depths behind the wall along the 15 feet cantilevered height of the wall. Table 4.1 and Figure 4.1 show the location of the 20 TDR probes in the ground. Physical moisture samples, taken periodically using a hand auger, will supplement the measurements obtained by the TDR probes.

Table 4.1: Location of the TDR probes installed in the soil

Probe #	Depth below Ground Surface (feet)	Distance Behind the Wall (feet)
1	1	20
2	1.75	1
3	13.5	1.6
4	1.5	1
5	0.9	1
6	0.5	10
7	3.7	5.2
8	13.6	1.7
9	6	3.5
10	2.5	1.7
11	9.2	1.8
12	1.8	1.9
13	1.5	4.9
14	5.8	5.3
15	5.1	0.9
16	0.9	10
17	1.75	1
18	0.5	1
19	0.5	1
20	0.5	20

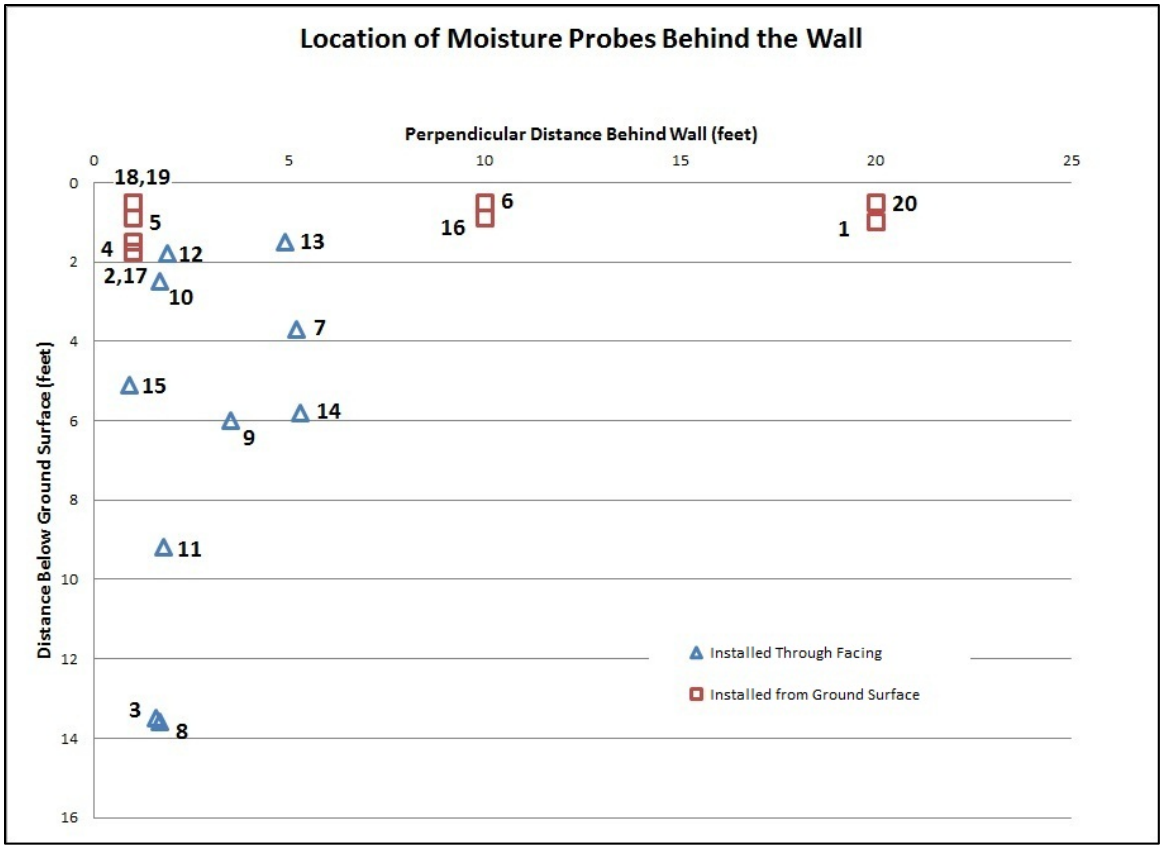

Figure 4.1: Location of the 20 TDR probes installed behind the wall

4.1.1: WATER TABLE MEASUREMENTS

The piezometer has been used to take records of the approximate location of the water table near the wall. This 1.25 inch diameter piezometer is grouted at the base of the borehole. The screen is located between five and 20 feet and the water level was determined using an electronic water level meter. Analysis of an initial rising head test that was performed over a period of weeks produced a saturated hydraulic conductivity of approximately 10^{-8} cm/sec. Since the piezometer has been installed, the depth to water has ranged from 7.5 feet below the ground surface (April 2010) to approximately 9.5 feet

below the ground surface (June 2011). While the water table in the area is most likely not at the same depth as the piezometer, the piezometer should give a good indication of what the water level is near the wall. The excavation of the wall has caused the water level to be affected. Small amounts of water can consistently be seen at the bottom of the excavation near the wall. Elevations taken from a pond on the owner's site show an elevation difference of approximately two feet.

4.1.2: TDR System Enclosure

The instruments needed to be enclosed on site in a box that can withstand the weather conditions. Historical temperature data has shown that yearly highs and yearly lows can vary up to 100 degrees Fahrenheit, with typical temperature above 100 degrees Fahrenheit in the summer and below freezing in the winter. Thunderstorms and large rainfall events are common, which means lightning protection is necessary. The site is limited to one AC power cord to run the instruments on site which consists of the TDR system and the optical strain gauge system.

In order to meet the onsite needs, the TDR operating system was placed in a NEMA 4 steel enclosure. The AC power cord runs from the on site power source to the box containing the optical strain gauge equipment. In this box, a surge protector is used to power both the optical strain gauges and a TDR system by a power cord leading to the TDR enclosure. From the optical strain gauge enclosure, the power cord then goes to a trickle charger in the TDR enclosure connected to a 12 Volt battery to keep the battery charged. The battery is connected to the TDR100 which powers the TDR system. In case the power goes out, the battery will be able to keep the system working until the power is back on. A lightning module is connected within the system to protect the system if stuck by lightning and the system is grounded to one of the rebar cages in an

non-instrumented shaft. The cables entering and leaving the box were waterproofed by using cable glands and heavy duty tape. Figure 4.2 shows the system within the NEMA 4 steel enclosure.

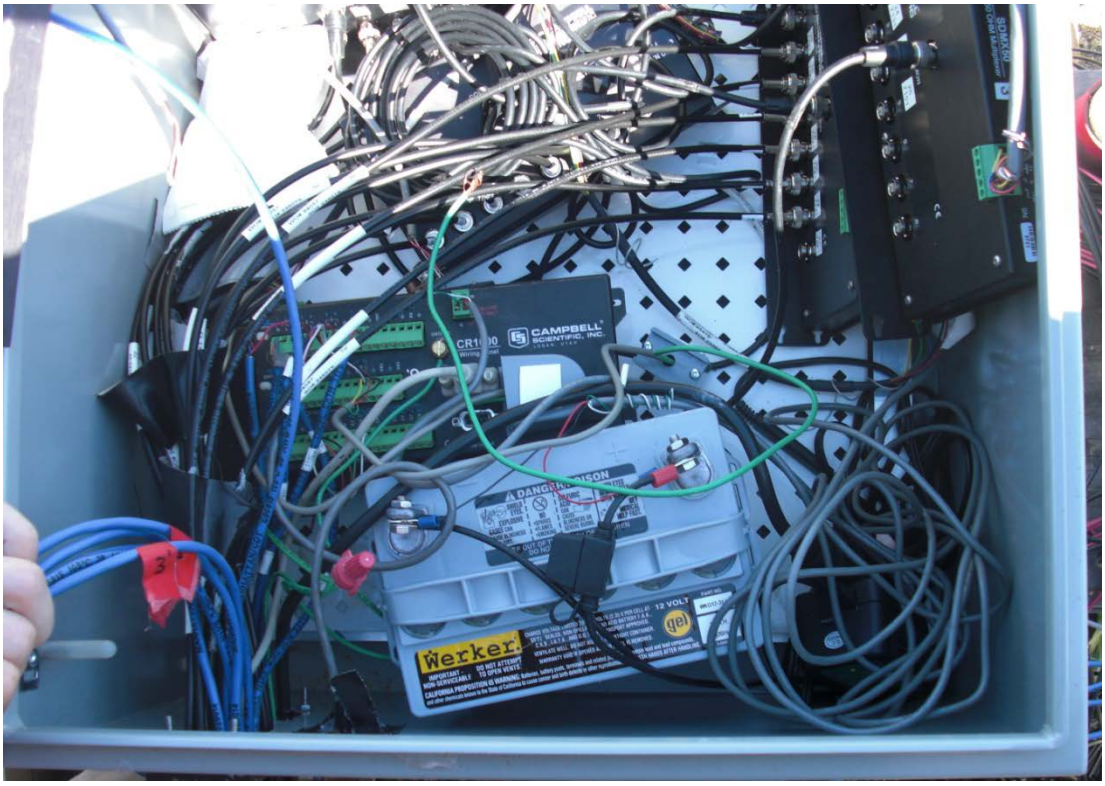

Figure 4.2: TDR system within the NEMA 4 steel enclosure

4.2: Set-up

The TDR probes were set up to record data on the Campbell CR1000 datalogger. The program on the CR1000 stores the probe constants and probe offsets in order to provide partially reduced data as an output. The measurement plan consists of recording electrical conductivity measurements and L_a/L measurements every 15 minutes and

recording full waveforms for each probe every two hours. The capacity of the CR1000 requires these data to be downloaded every two to three weeks.

As mentioned in Chapter 2, the L_a/L values are taken from the waveform using an algorithm from the TDR100. The L_a/L is calculated from the waveform, stored on the CR1000, and the waveform is discarded. Having L_a/L allows for the dielectric constant (K_a) to be calculated. The equation (Equation 2.6) from Topp et al. (1980) allows for the moisture content to be determined empirically.

The full waveforms are only taken every two hours due to the amount of memory space waveforms fill. Each waveform consists of 251 points that need to be stored for each probe. Having full waveforms allow for the L_a/L values to be checked or calculated if there is a issue with the algorithm reading the correct points on the waveform.

4.3: Probe Constant Calibration

The calibration of the TDR system was performed at Ensoft, Inc. in Austin, Texas. These calibrations were performed in accordance with the TDR 100 Manual (Campbell Scientific, Inc., 2010). The calibration process was done using PCTDR-Version 2.07 from Campbell Scientific, Inc.

4.3.1: Probe Constant Calibration

The probe constant (K_p) is required for the measurement of electrical conductivity. The calibration procedure and equations used were obtained from TDR100 Manual (Campbell Scientific, Inc., 2010). Electrical conductivity is calculated using Equation 4.1.

$$\sigma = K_p * G \qquad \text{(Equation 4.1)}$$

Where σ is electrical conductivity and G is the electrical conductance. The probe constant is the ratio of the electrical conductivity to the electrical conductance. By immersing the TDR probes in a solution of known electrical conductivity and measuring the electrical conductance, the probe constants can be determine. Distilled water mixed with a specified amount of Potassium Chloride (KCl) was used as the solution with known electrical conductivity. The electrical conductance is determined by Equation 4.2 (Campbell Scientific, Inc., 2010).

$$G = \left(\frac{1}{Z_u}\right)\left(\frac{1-\rho_{corrected}}{1+\rho_{corrected}}\right) \qquad \text{(Equation 4.2)}$$

where Z_u is the system impedance (50 ohms) and $\rho_{corrected}$ is the corrected reflection coefficient. The corrected reflection coefficient is calculated using Equation 4.3 (Campbell Scientific, Inc., 2010).

$$\rho_{corrected} = 2\left(\frac{\rho_{uncorrected}-\rho_{open}}{\rho_{open}+\rho_{shorted}}\right) \qquad \text{(Equation 4.3)}$$

where $\rho_{uncorrected}$ is the uncorrected reflection coefficient measurement, ρ_{open} is the reflection coefficient measured when the probes are left in air, and $\rho_{shorted}$ is the reflection coefficient measured when the probe rods are shorted. The probes were shorted by firmly covering the probe rods with a hand (Campbell Scientific, Inc., 2010).

Using Equations 4.1-4.3 and following the directions provided by the TDR100 Manual (Campbell Scientific, Inc., 2010), the probe constants were found for each probe.

The process was performed using the program, PCTDR-Version 2.07 from Campbell Scientific, Inc.

During this calibration of the probe constants, the waveform settings are determined for each probe. Figure 4.3 shows the screen that is used when calibrating with the PCTDR-Version 2.07 from Campbell Scientific Inc. The number of points used to define the waveform is entered into the program. The standard number of points used to define the waveforms by Campbell Scientific, Inc. is 251. The window that shows the waveform has to be adjusted for each probe. This window is determined by the cable lengths from the TDR100 to the probe.

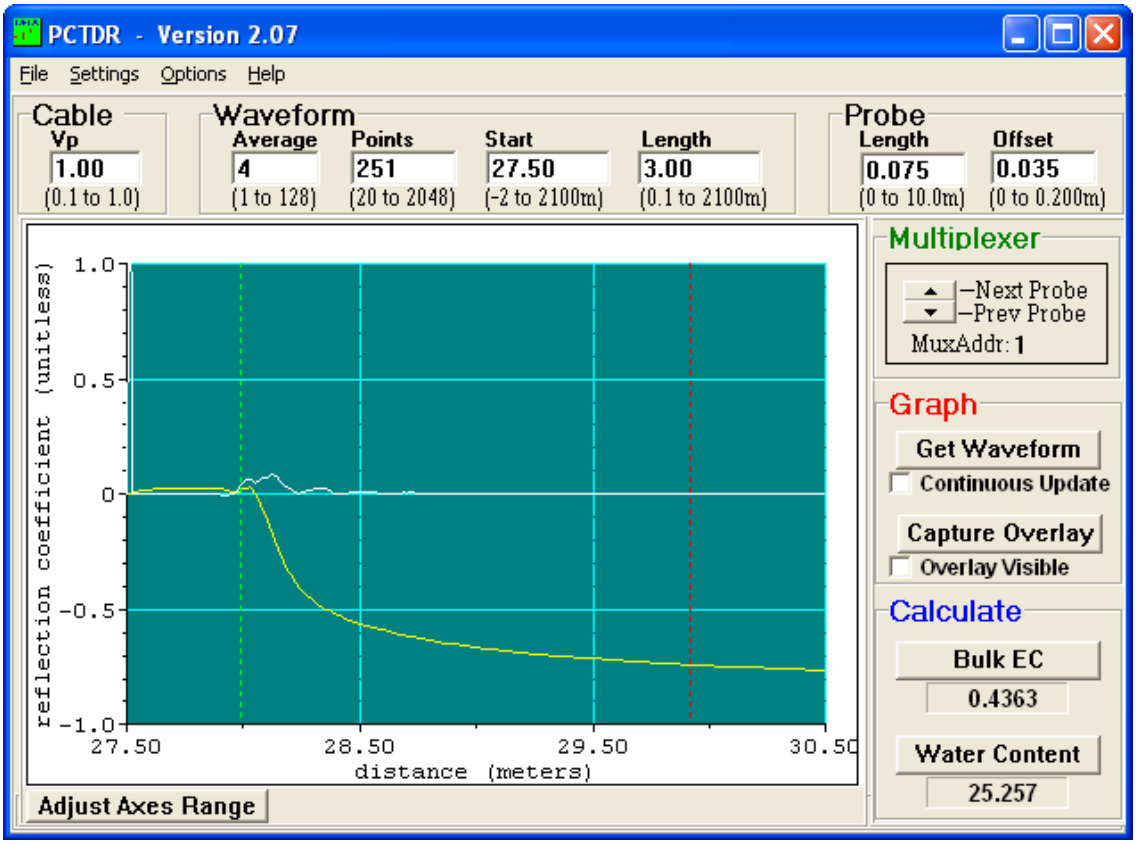

Figure 4.3: PCTDR-Version 2.07 calibration screen

4.3.2: PROBE OFFSET CALIBRATION

Part of the TDR rods of the probe are enclosed by the head material and thereby not exposed to the soil when installed in the ground. In order to account for this in the calculations, a probe offset is needed. A procedure for calibrating each probe's offset is described in the TDR100 Manual (Campbell Scientific, Inc., 2010).

This calibration was not done for the probes in this project, however. This decision was made after a phone conversation with Glenn Jarell from Campbell Scientific Inc. (2010). The reason for not calibrating the offset is that Campbell manufacturing tolerances are tight enough that there is more uncertainty associated with the calibration process than just using the specification values provided by Campbell Scientific, Inc. (Jarell 2010). The specification offset value for the Campbell Scientific Inc. CS645-L probes is 0.035 meters.

4.3.3: SOIL SPECIFIC CALIBRATION

The reason to do a soil specific calibration is to define the sensor behavior for the specific soil that the instrument is being used in. In many cases TDR probes do not need a soil specific calibration for accurate data to be produced. However, Topp et al. (1980), Jones and Or (2004), Reedy and Scanlon (2002) and several others found that the TDR probes become inaccurate in soils with a high electrical conductivity.

The issues with performing a soil specific calibration at the project site are that the soil is highly overconsolidated and has a high occurrence of fissures and dense soil blocks. Reproducing the in situ soil conditions is very difficult in the lab. The Taylor Clay also has a high Plasticity Index which presents a problem when performing a soil specific calibration. Reedy and Scanlon (2002) had difficulty performing a soil specific calibration for a clay with a high Plasticity Index.

Campell Scientific, Inc. Tech Support, (2010) suggested that performing a soil specific calibration for the TDR probes on the project was probably not necessary. The reason for not doing soil specific calibration was because, in their experience, it was more likely that a mistake made during calibration would cause more inaccuracies than just using the Topp et al. (1980) equation. If there was a problem, electrical conductivity and the waveforms could be used to determine the water content of the soil. Due to the difficulty of performing a soil specific calibration, construction time constraints, and conversations with Campbell Scientific Inc. Tech Support (2010), a soil specific calibration was not done for the TDR probes on this project.

CHAPTER 5: TDR PROBE INSTALLATION

The installation of the TDR probes into the soil on site is described in this chapter. Installation of the probes occurred in two stages. On September 30 and October 1, 2010, 10 probes were installed through the facing of the wall. On October 14, 2010, the remaining 10 probes were installed from the ground surface. Monitoring of the probes started immediately after they were installed. The layout of the 20 probes is shown in Figure 5.1.

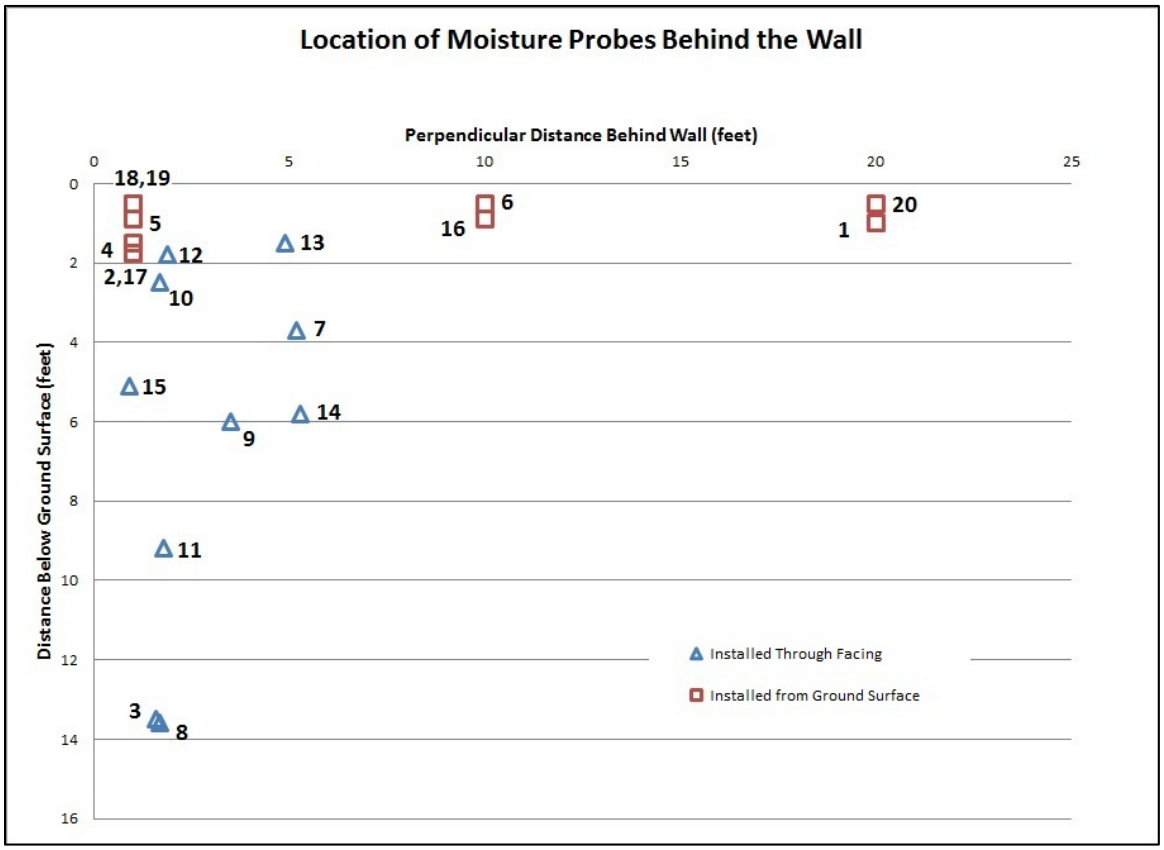

Figure 5.1: Location of the 20 TDR probes installed behind the wall

5.1: Installation of Sensors through the Wall Facing

The sensors installed through the facing of the wall were placed on September 30 and October 1, 2010. This was done before the shotcrete facing on the wall was placed in the afternoon of October 1, 2010. The facing of the wall was put on by Craig Olden, Inc.

Figures 5.1 and 5.2 show the layout of the probes placed through the facing of the wall. Probes were placed at a depth of 1.5 feet to 13.5 feet below the ground surface and at a distance of 0.9 feet to 5.3 feet behind the wall. Table 5.1 shows the depth below the ground surface and the distance behind the wall of each of the probes installed through the facing of the wall. Figure 5.3 shows one of the probes installed through the facing of the wall.

Table 5.1: Location of the probes installed through the facing of the wall

Probe #	Depth below Ground Surface (feet)	Distance Behind the Wall (feet)
3	13.5	1.6
7	3.7	5.2
8	13.6	1.7
9	6	3.5
10	2.5	1.7
11	9.2	1.8
12	1.8	1.9
13	1.5	4.9
14	5.8	5.3
15	5.1	0.9

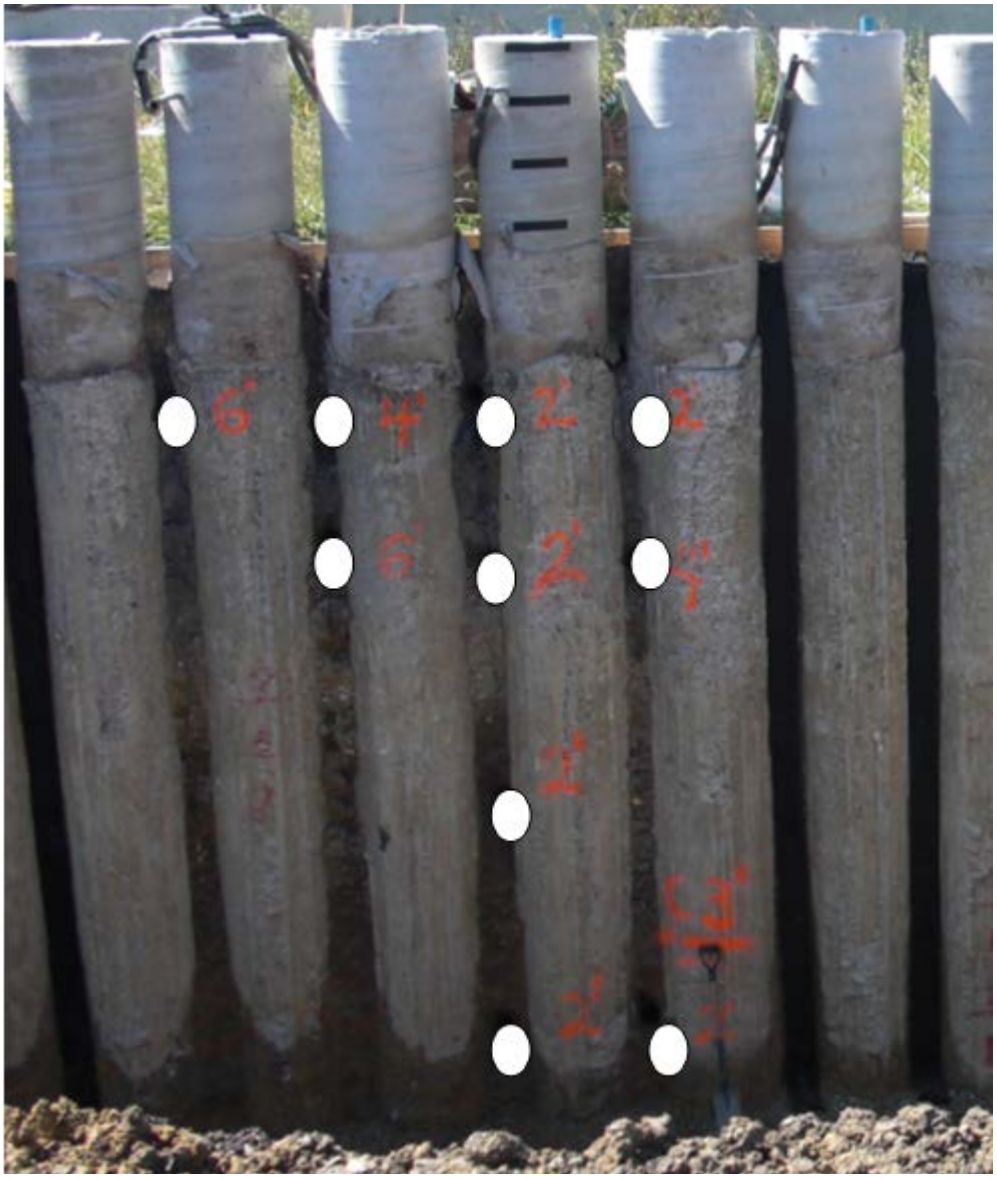

Figure 5.2: Layout of TDR probes installed through the facing of the wall

Figure 5.3: A sample installation of a probe installed through the facing of the wall

Figure 5.4: A hole being drilled by Craig Olden, Inc

The ten holes to place the probes in the soil were drilled by Craig Olden, Inc. using a soil nail rig. Each hole was drilled with an angle of approximately 15 degrees from horizontal. Figure 5.4 shows Craig Olden, Inc. drilling one of the holes for the probes.

In the locations the probes could not be installed by hand, the probes were pushed into the soil using a slotted PVC pipe. Once the probe was in place, the hole was backfilled with dry native clay from the site. The holes were backfilled with native dry clay so the soil would swell and fill the voids when the water reached the dry soil. The dry clay fill was tamped into place and sealed with a wet clay to hold the fill until the shotcrete was placed.

The cables from the TDR probes were protected from damage from the shotcrete impact by placing the cables in slotted PVC pipes. Tape and cable ties were used to keep the cables within the PVC pipe and the slotted side was faced towards the inside of the wall to prevent the shotcrete from directly hitting the cables. Figure 5.5 shows the cables being protected by the PVC pipe.

Figure 5.5: The PVC pipe protection for the TDR probe cables to minimize damage from the shotcrete

5.2: Installation of Sensors from the Ground Surface

The sensors that were installed through the ground surface behind the wall were placed on October 14, 2010. Ten probes were installed at depths from 0.5 feet to 1.75 feet and at a distance of one foot to 20 feet behind the wall. Table 5.2 shows the depth below the ground surface and the distance behind the wall of each of the probes installed through the ground surface.

Table 5.2: Location of the probes installed from the ground surface

Probe #	Depth below Ground Surface (feet)	Distance Behind the Wall (feet)
1	1	20
2	1.75	1
4	1.5	1
5	0.9	1
6	0.5	10
16	0.9	10
17	1.75	1
18	0.5	1
19	0.5	1
20	0.5	20

The holes for these probes were dug for the first foot by using a pick axe since there is an initial layer of base course on site that was stiff and difficult to excavate. For the probes that were deeper than one foot, a drill with a custom drill bit, made by owner of site, was used to reach the desired depths. Once the probes were placed in the soil, the holes were backfilled with the dried native clay soil so the fill would swell and fill the voids when wetted. Figure 5.6 shows one of the probes installed in the ground before the dried native clay fill was placed.

Figure 5.6: A sample probe installation from the ground surface.

5.3: Installation Problems

Site conditions made installation of the probes difficult. A large amount of force was required to push the probe rods completely into the soil because of the high shear strength of the highly overconsolidated Taylor Clay. Since the force required was large, it was more likely for air gaps to be created by accidental movement of the probe when trying to gain the necessary force to completely push in the probe rods. The use of the PVC pipe to install the probes in longer holes through the facing of the wall made it difficult to uniformly push the probe in the soil.

In some cases it was not possible to put enough force on the probes to push the probes completely into the clay. Figure 5.7 shows an example of a probe that could not be pushed completely into the clay. In these cases, the dried native clay fill was backfilled around the end of the probe and it was hoped that any air caps would close when the clay fill swelled.

The soil on site has many rocks and fossilized shells within it which could damage the probes when installed. Several probes were bent during installation. The rods were straightened when noticed but it was not possible to detect if the rods of the probes had deviated by hitting a rock or shell in the clay once pushed into the soil. Also, when installing the probes into deep holes, there was no way to verify if the probe was installed with the rods in the correct orientation.

Tests by Campbell Scientific Inc. showed only 0.03 percent change in the results when the probes were deflected four millimeters (Brown 2011). However, it was noted that the tests were performed in air and water so the results could differ in soils due to the causing of air gaps or the soil compacting. It is possible that the rods deviated by more than four millimeters when installed into the soil. Some of the rods that were bent during installation and fixed had deviated by more than four millimeters.

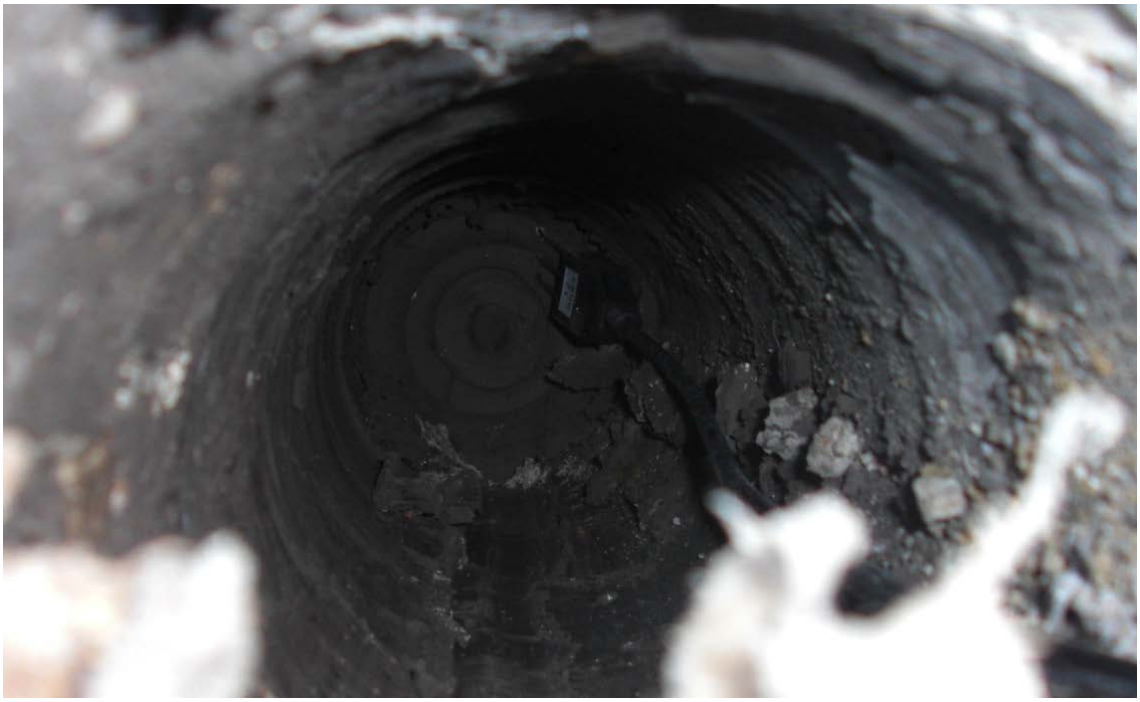

Figure 5.7: A sample probe installation where the probe could not be pushed completely into the soil

CHAPTER 6: FIELD PERFORMANCE

The moisture measurements taken and performance of the TDR probes are described in this chapter. Also, the possible problems and potential solutions are discussed.

6.1: Moisture Measurements

Since the site investigation, moisture samples have been taken in the upper six feet of the Taylor Clay near the wall. The moisture contents in the upper six feet have ranged from approximately 35 percent to approximately 17 percent. Figure 6.1 shows the moisture contents taken since the site investigation in January 2011. The moisture contents that are labeled M-7B are moisture contents taken after an eight hour inundation test was perform in an area away from the wall. This inundation test was done by ponding water at a head between two and six inches.

Also in Figure 6.1 are the ground water measurements taken from the piezometer near the wall. On February 16, 2010, the piezometer was bailed out to a depth below ground surface of 19 feet for a rising head test to be performed. By June 2010, the water level had risen to a depth of 7.5 feet below the ground surface. Since June 2010, the water level has gradually fallen to a depth of 9.5 feet below the ground surface in June 2011. This decrease in the water level since June 2010 correlates with the lack of rainfall that the area has experienced. Figure 6.2 shows the daily precipitation data from January 2008 to July 2011.

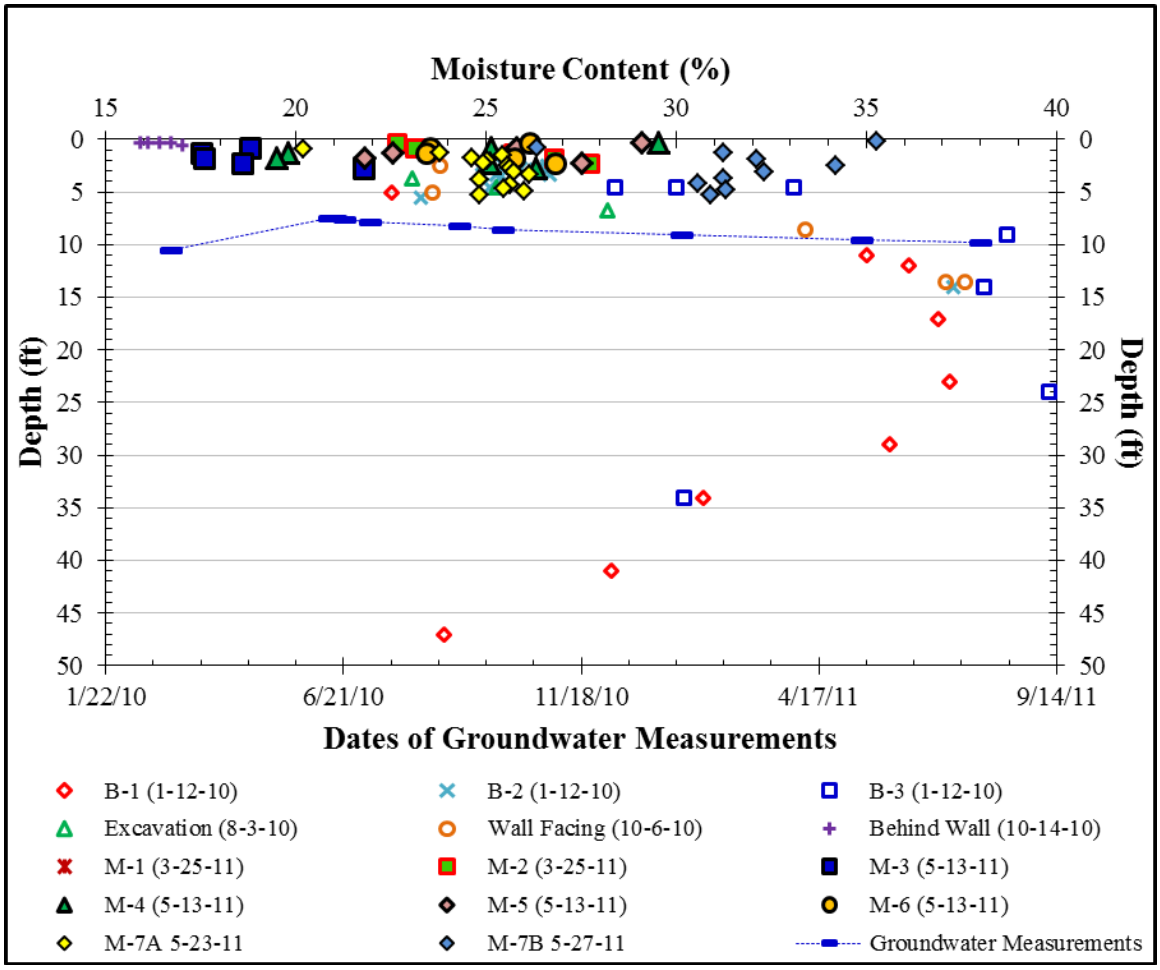

Figure 6.1: Moisture Measurements taken from January 2010 to May 2011 (Ellis 2011)

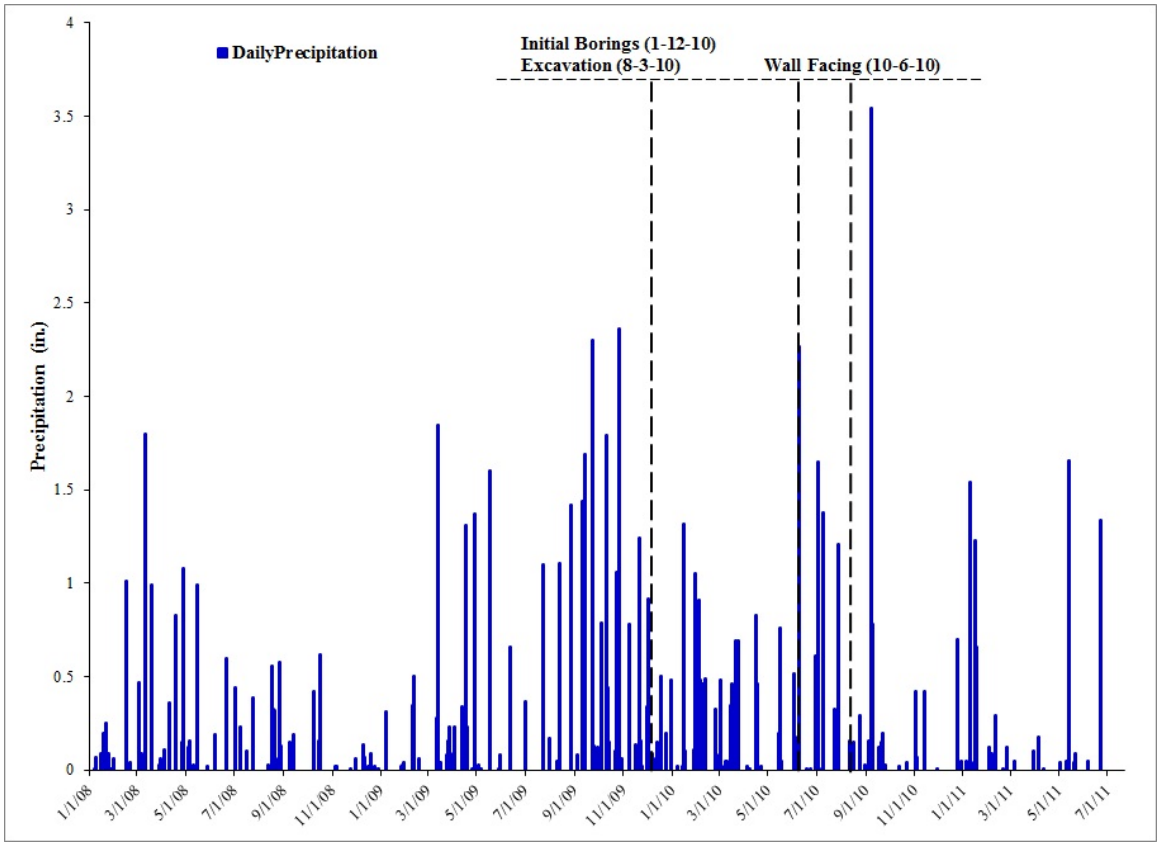

Figure 6.2: Daily precipitation measurements from January 2008 to July 2011 (Ellis 2011)

6.2: Performance

Initially, 15 probes were non-functional, four probes were semi-functional, and one probe was functional. For this study, non-functional means the probes were not giving data that indicate the probes are measuring the dielectric constant of the soil. Semi-functional probes are probes that are giving waveforms that are reasonable but with a large amount of noise. A probe that gives reasonable waveforms is classified as a functional probe for this study. Campbell Scientific, Inc. uses a computer algorithm to determine the L_a/L values from the waveforms. The use of L_a/L data to analyze the

waveform was not possible due to an inability of the computer algorithm to read the correct points of the waveforms. A large amount of scatter was seen in the electrical conductivity measurements.

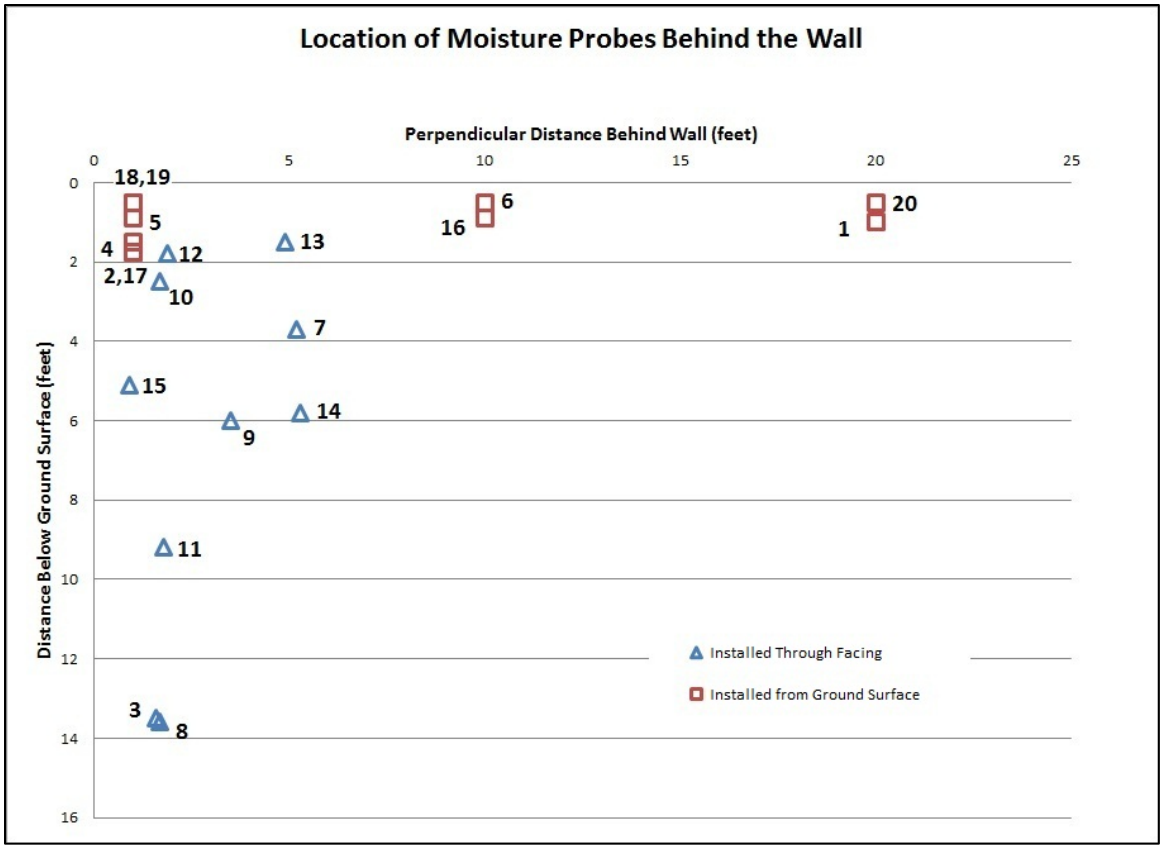

Figure 6.3: Location of the 20 TDR probes installed behind the wall

6.2.1: FUNCTIONAL PROBE

Probe 4 (Figure 6.3) was the only probe that was fully functional and is located at a depth of 1.5 feet below the ground surface and one foot behind the wall. Electrical conductivity measurements from Probe 4 are shown in Figure 6.4. Initial electrical conductivity data show a wide band of values ranging between 13 and 26 Siemens/meter.

Based on a conversation with Robert Reedy (2010) of the University of Texas at Austin Bureau of Economic Geology, electrical conductivity measurements are more robust than L_a/L measurements for soils of this type, and can be correlated with moisture content. However, the data here varies too much to usefully correlate the electrical conductivity to the moisture content of the soil. Also, the TDR probes for this study have a manufacturing specification of a maximum electrical conductivity of 0.5 Siemens/meter, which could be a reason for the large amount of scatter (Campbell Scientific, Inc., 2010). Patterson and Smith (1985), Campbell Scientific, Inc. (2010), Reedy (2010), and several others also indicated that better measurements would come from a combination of shorter cable lengths and longer probe lengths, which is not the situation for this project (70 feet cables and 2.95 in probes).

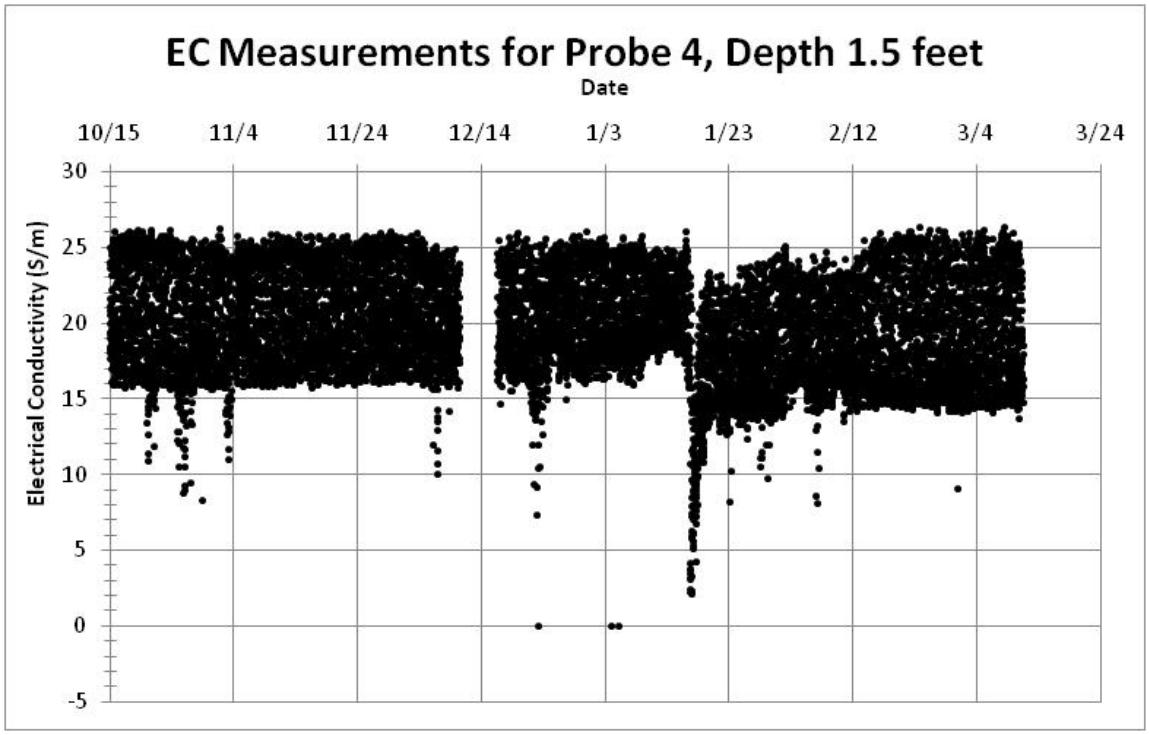

Figure 6.4: Electrical conductivity measurements for Probe 4

Daily temperature cycles of the electrical conductivity are expected since the electrical conductivity is temperature dependent. The electrical conductivity increases with increasing temperature. However, closer analysis of the electrical conductivity does not show any daily variation with temperature. Closer analysis of data over a 24 hour period on March 3, 2011 shows a large amount of scatter and no clear temperature dependence (Figure 6.5)

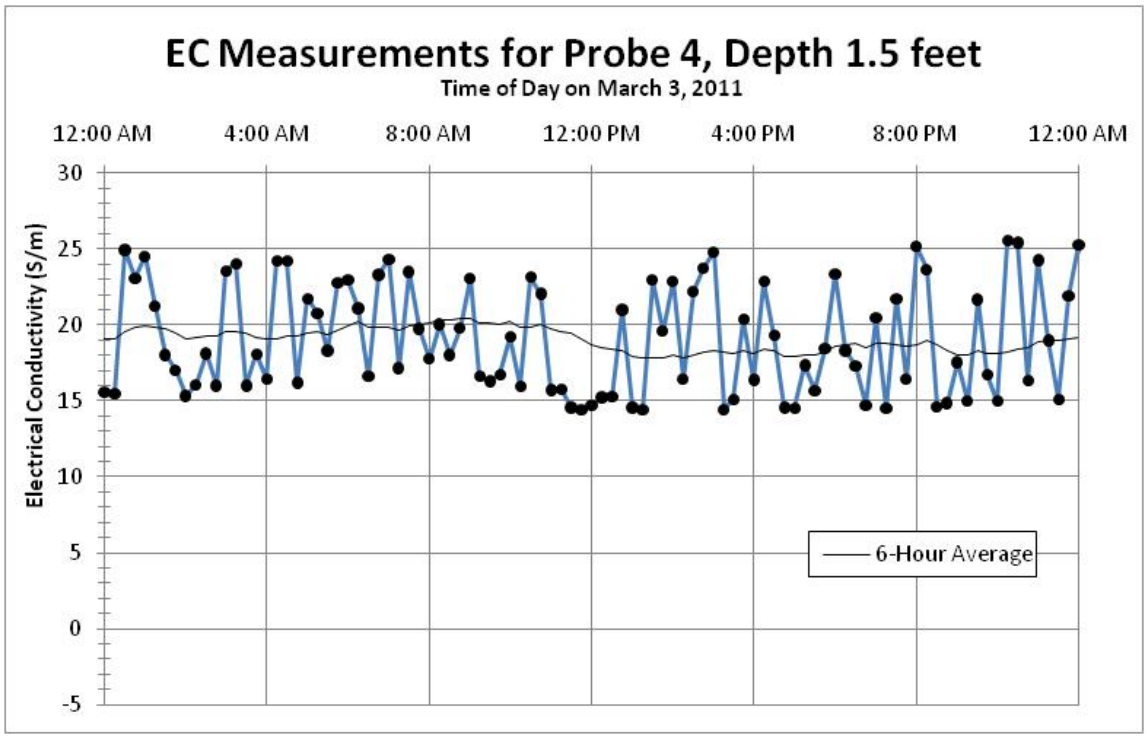

Figure 6.5: Electrical conductivity measurements over a 24 hour period on March 3, 2011.

The L_a/L data for this functional probe has not been giving good measurements. Data show up as separate bands of measurements (Figure 6.6). This result was due to the inability of the computer algorithm to find the points at the beginning and end of the

probe. Since the computer algorithm could not find the necessary points on the waveform, it is necessary to manually inspect the waveform.

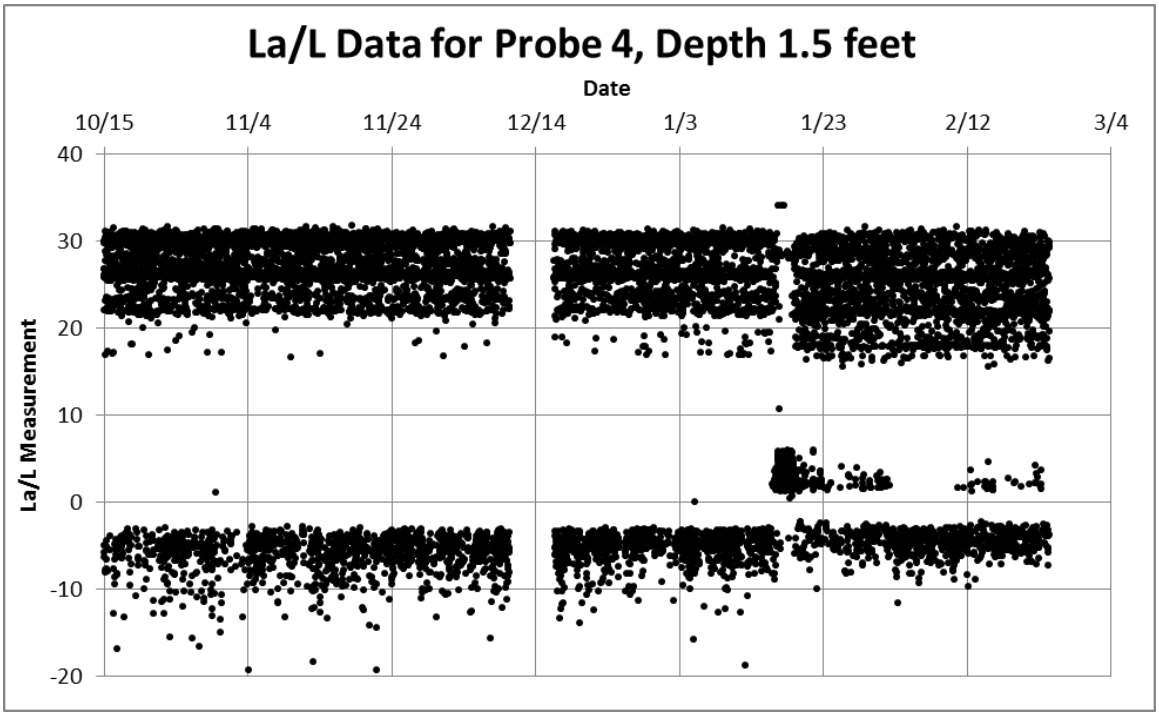

Figure 6.6: La/L data for Probe 4 inferred by the Campbell Scientific, Inc. algorithm

The waveform data for the functional probe is the most useful data that has been received from any of the waveforms. Figure 6.7 shows waveforms from the functioning probe. The waveforms for this probe show some AC noise but the shape is clearly visible.

These waveforms show the probe is measuring the soil but due to attenuation of the signal, the waveform does not show the reflection point indicating the end of the probe. This is most likely due to the high electrical conductivity of the soil and the long cable lengths. Figure 6.8 and 6.9 show an example the effects of differing cable lengths

and high electrical conductivity in a sandy loam. The waveforms look like the waveforms in soils with high electrical conductivity described in the TDR100 Manual Campbell Scientific, Inc. (2010). Reedy and Scanlon (2002) also observed these types of waveforms in soils with a high electrical conductivity without the second peak (point 3). They were unable to use the waveforms so Reedy and Scanlon (2003) correlated the moisture measurements to electrical conductivity values.

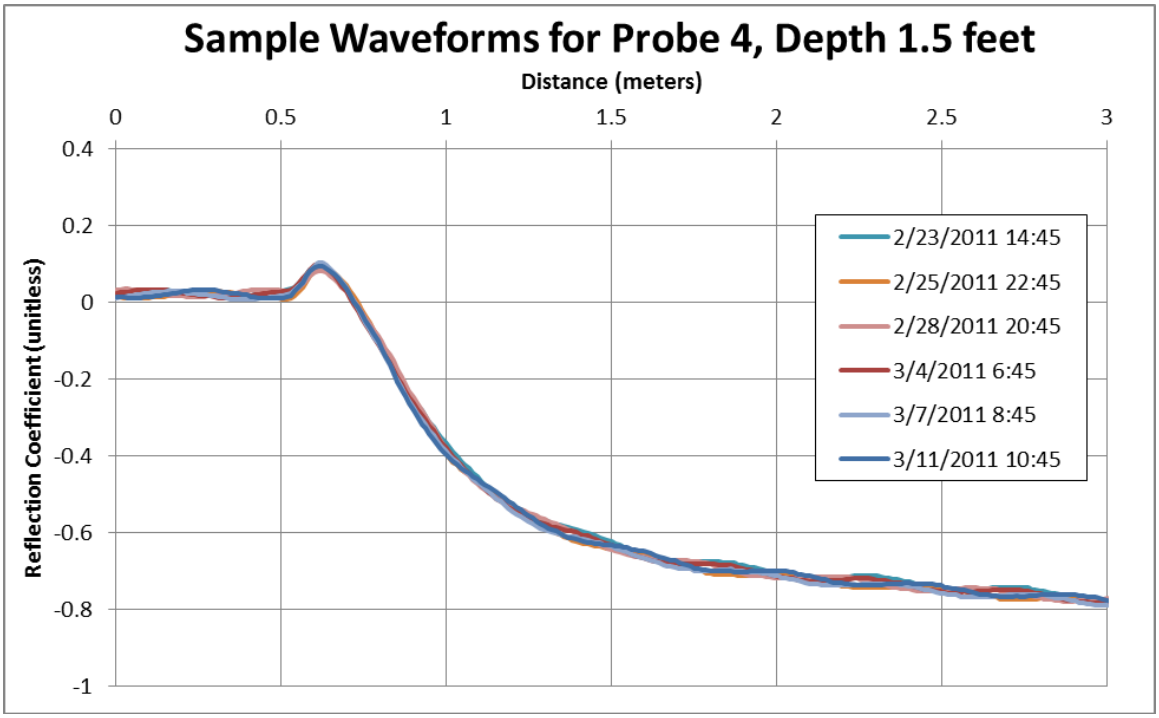

Figure 6.7: Waveform data for the functioning probe

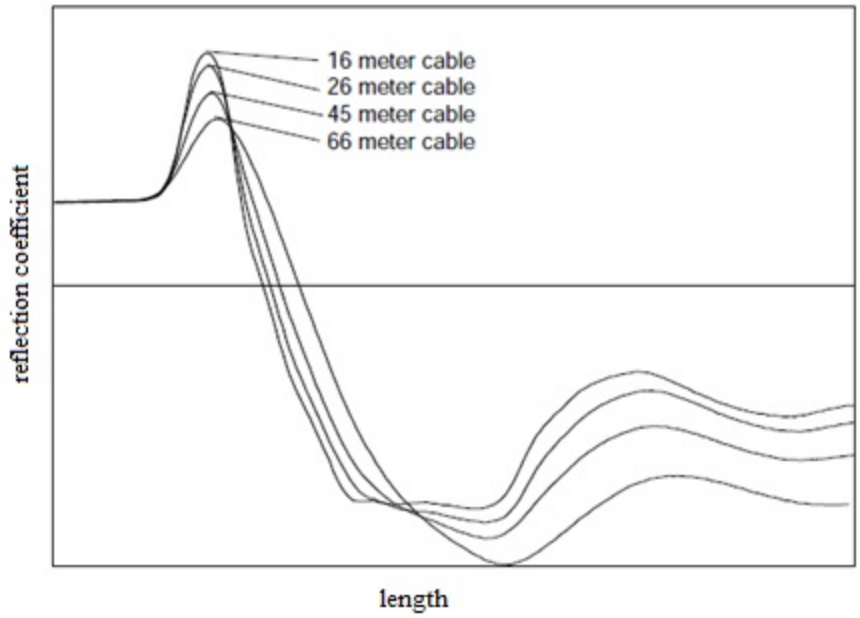

Figure 6.8: Waveforms for differing cable length in a sandy loam (Campell Scientific, Inc., 2010)

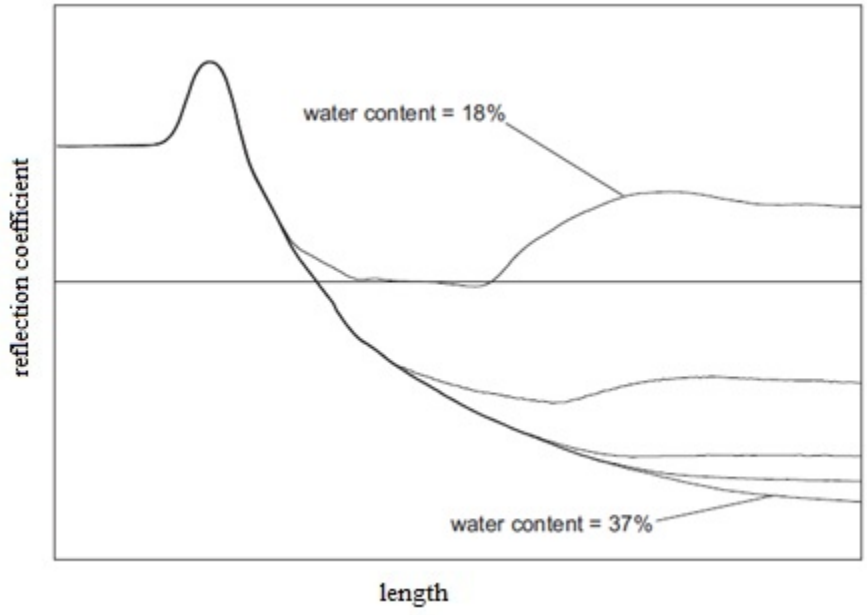

Figure 6.9: TDR waveforms in a sandy loam with a high electrical conductivity of 10.2 dS/m (Campell Scientific, Inc., 2010)

6.2.2: SEMI-FUNCTIONAL PROBES

Probes 7, 9, and 10 (Figure 6.3) have been semi-functional and Probe 16 was initially semi-functional but became non-functional in January 2011. The electrical conductivity data for these semi-functional probes show as a wide localized band of data typically between 10 and 30 Siemens/meter which is similar to Probe 4 which has values ranging from 13 to 26. This data follows the same pattern as the functional probe and shows no daily temperature cycles. Figure 6.10 shows the electrical conductivity data for Probe 9.

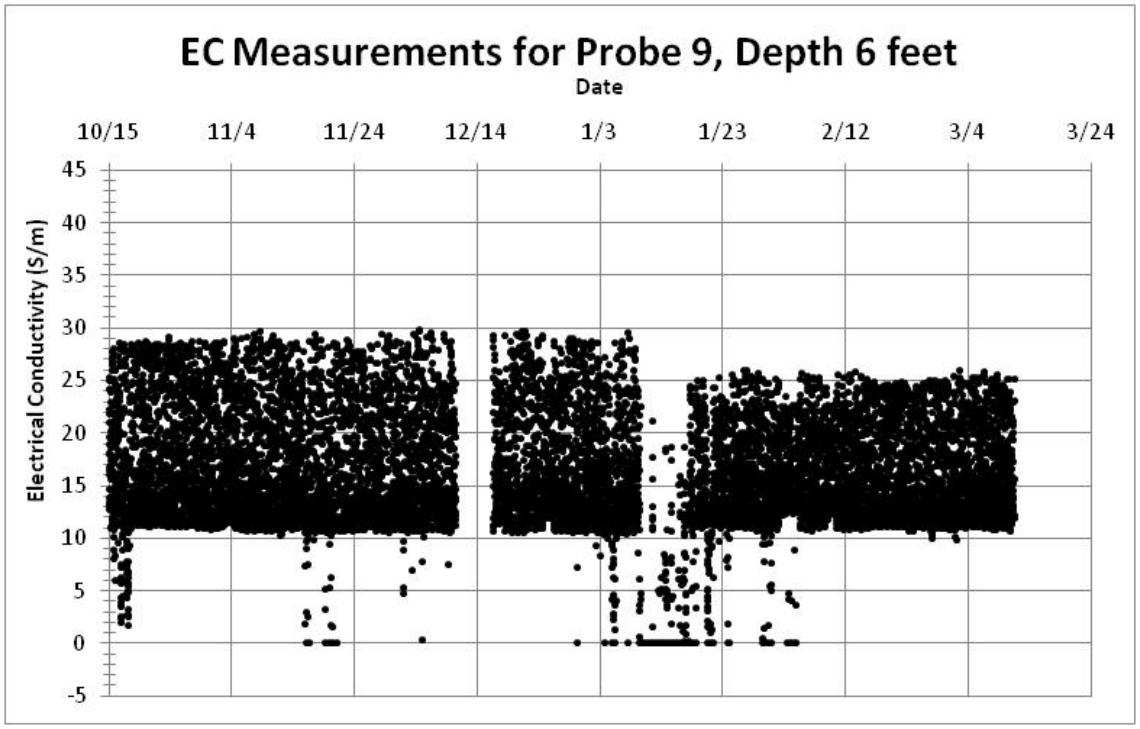

Figure 6.10: Electrical conductivity measurements for Probe 9

The automated inference of L_a/L for these probes provides no useful measurements. The data shows as distinct separate bands of measurements (Figure 6.11).

This result is due to the computer algorithm picking incorrect points from the waveforms that are showing a large amount of what appears to be AC noise.

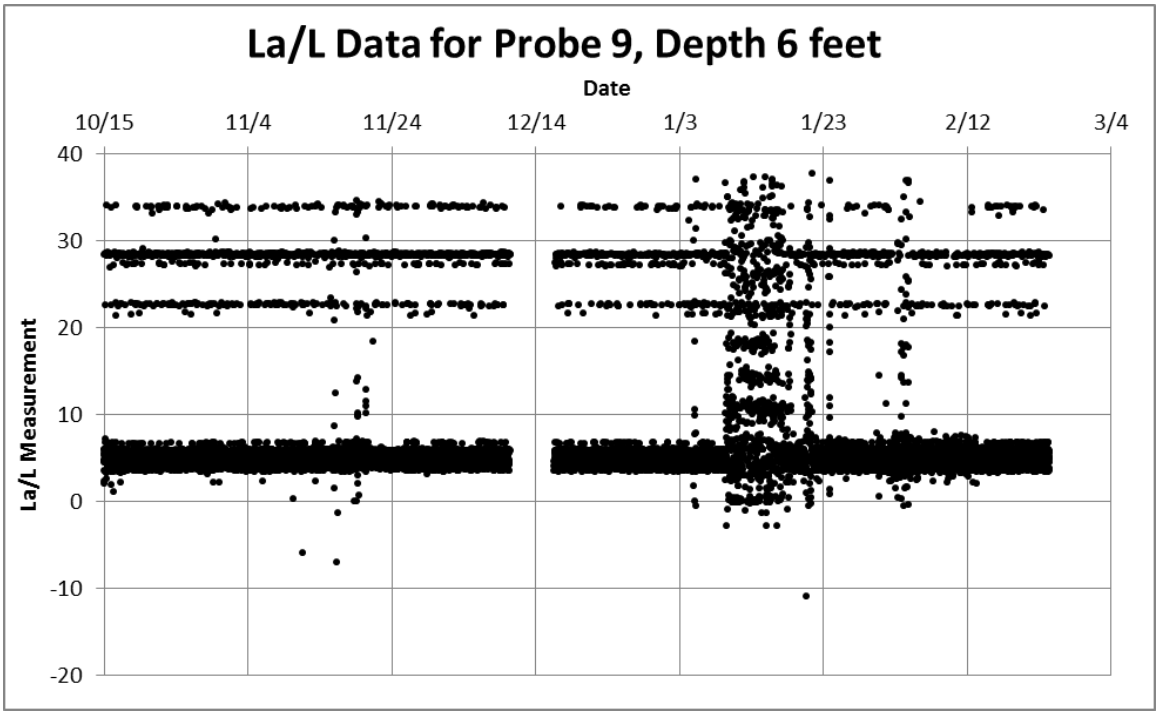

Figure 6.11: La/L data for Probe 9

The waveform data for the semi-functional probes is similar to the waveforms for the functional probe except there is a large amount of AC noise being seen in the waveform. Filtering the AC noise by using median waveform values over the period of one day was needed in order to get waveforms that do not show as much AC noise. Figure 6.12 shows a sample waveform from Probe 9. The AC noise likely comes from the power cords that are used to run the monitoring system on site.

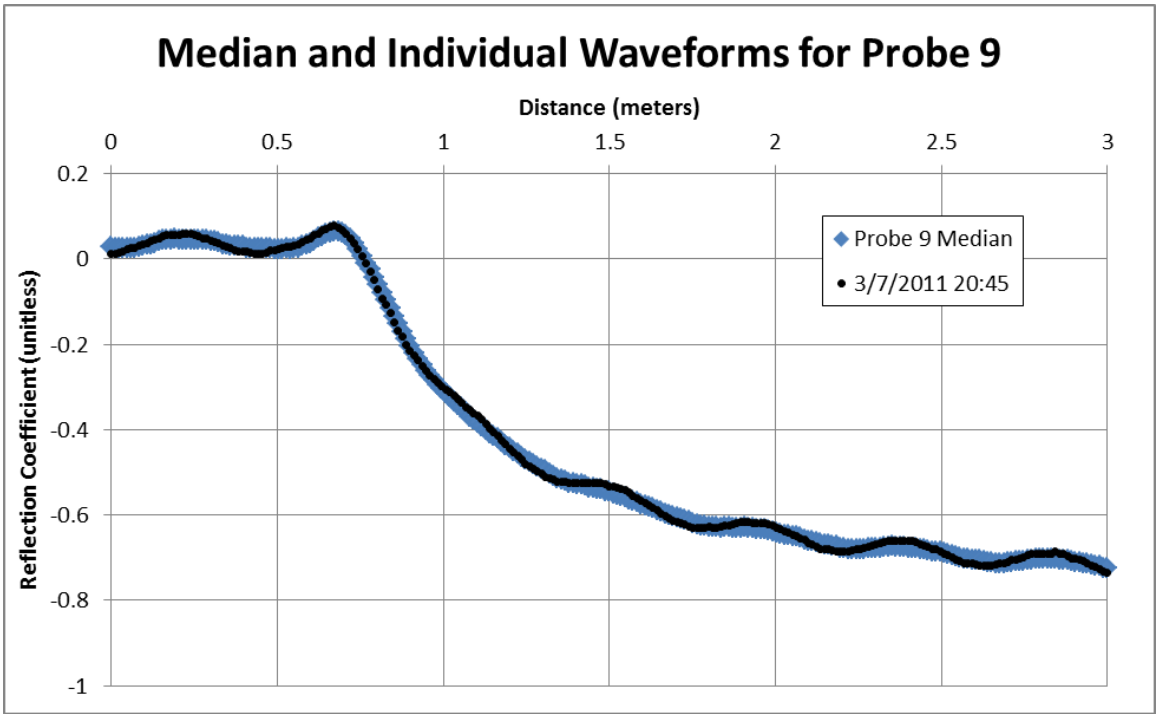

Figure 6.12: Sample waveforms from Probe 9

6.2.3: NON-FUNCTIONAL PROBES

Probes 1-3, 5-6, and 11-15, and 17-20 (Figure 6.3) have been non-functional since installation. As mention in the previous section, Probe 16 also became non-functional in January 2011. The data did not show values that would indicate the probes were measuring the properties of the soil. Data from the electrical conductivity measurements would often show that the TDR probe was not able to record a measurement for the soil. When the TDR probes did provide an electrical conductivity values, the values would range from -2 to 2 S/m. Electrical conductivity data ranged from -1.5 to 2. Other values that are seen are scattered values that are not reasonable. A possible reason for this result is that the probe rods do not have good contact with the soil. Electrical conductivity data from probe 15 is shown in Figure 6.13.

The inferred values of L_a/L show as distinct bands that have no apparent meaning since the waveform data is also not good (Figure 6.14). The waveform data also suggest that the probe rods could not have good contact with the soil as one of the best waveforms from these probes is shown in Figure 6.15. These data appears to show AC noise that could possibly come from the power cords on site.

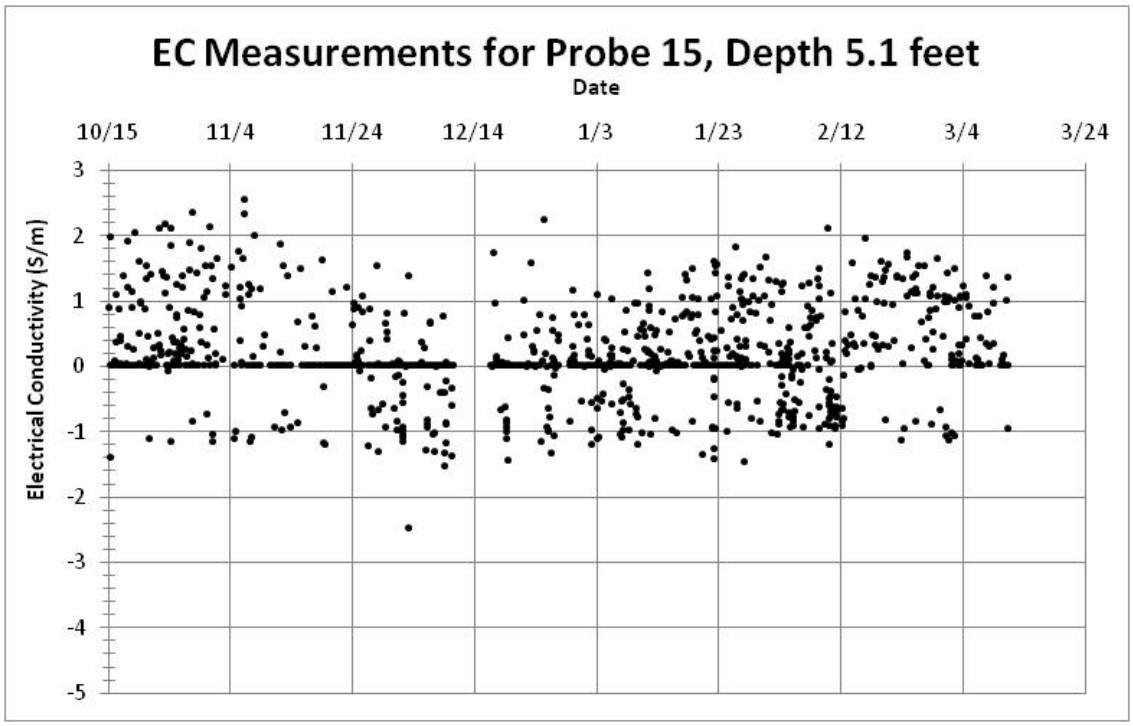

Figure 6.13: Electrical conductivity data from Probe 15

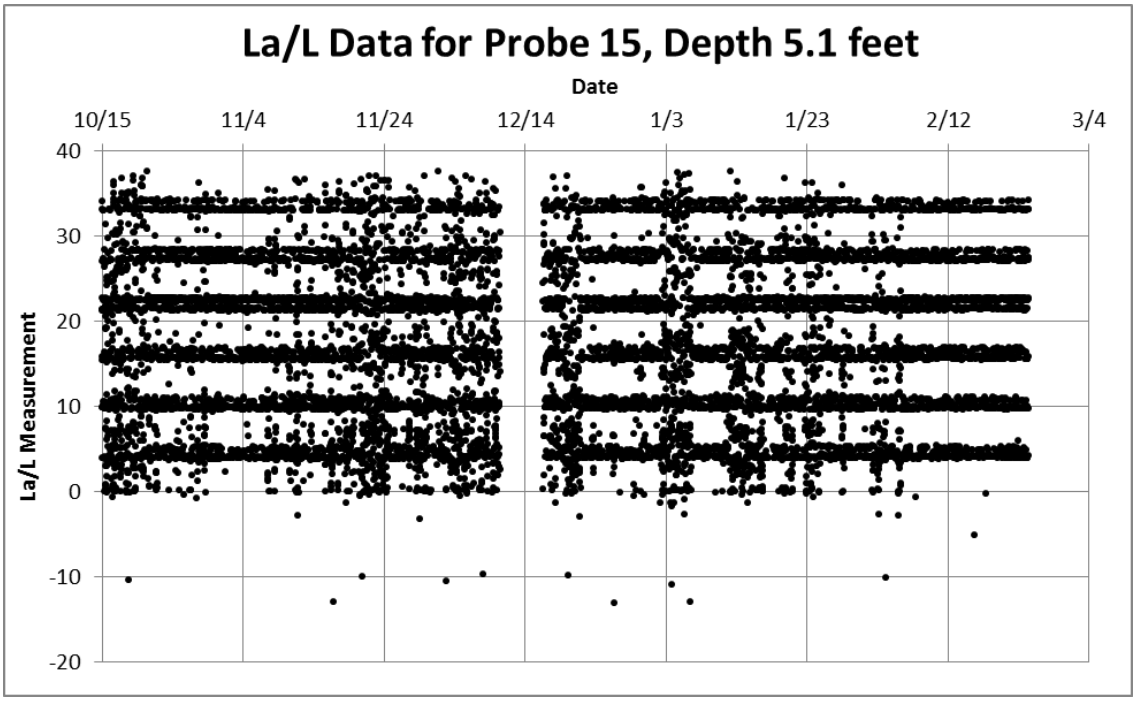

Figure 6.14: La/L data from Probe 15

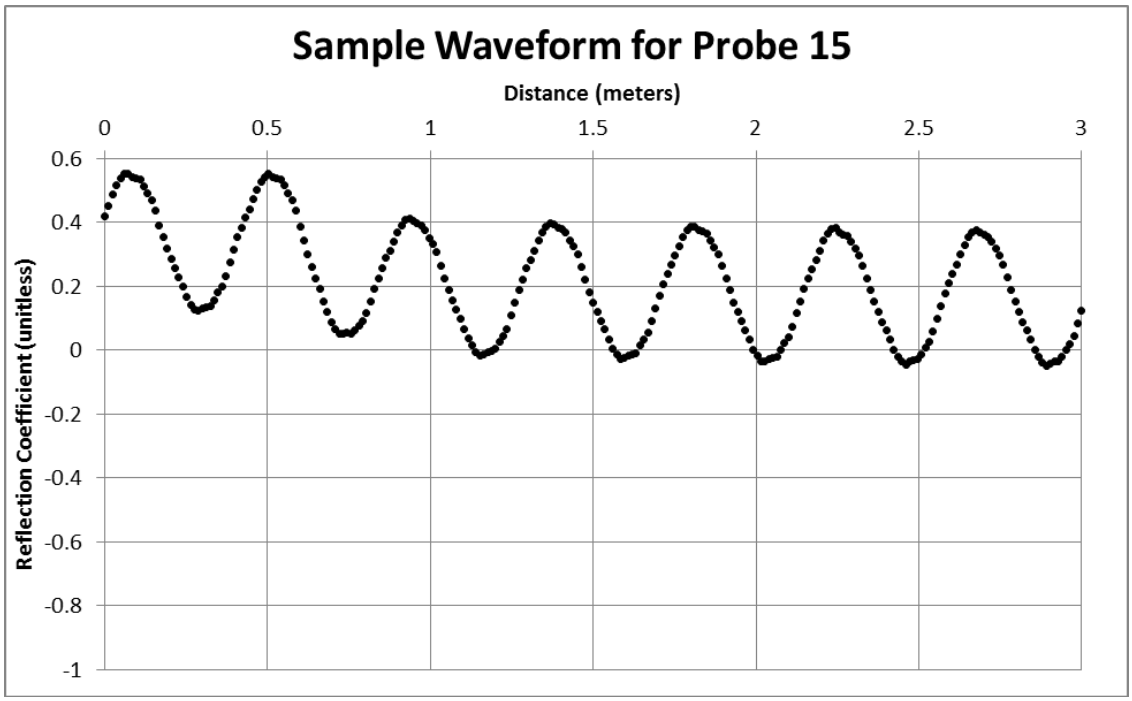

Figure 6.15: A sample waveform from Probe 15

6.2.4: RAINFALL EVENTS

From installation of the probes in October 2010 to January 2011, there was no significant rainfall. Approximately three total inches of rain fell in two events on January 9 and January 16, 2011. On these dates, many of the sensors show a change in data and in some cases the change stayed constant. Each of the semi-functional probes and the functional probe showed a change in the electrical conductivity data. Those changes can be seen in Figures 6.4, 6.10 and 6.16.

It was during these events that the semi-functional Probe 16 became nonfunctional. Based on email correspondence with Glenn Jarrell and Jason Ritter of Campbell (Jarell and Ritter 2011), the most likely reason for the change is an increase of electrical conductance of the soil due to a change in the moisture content. The electrical conductivity data for Probe 16 is shown in Figure 6.16.

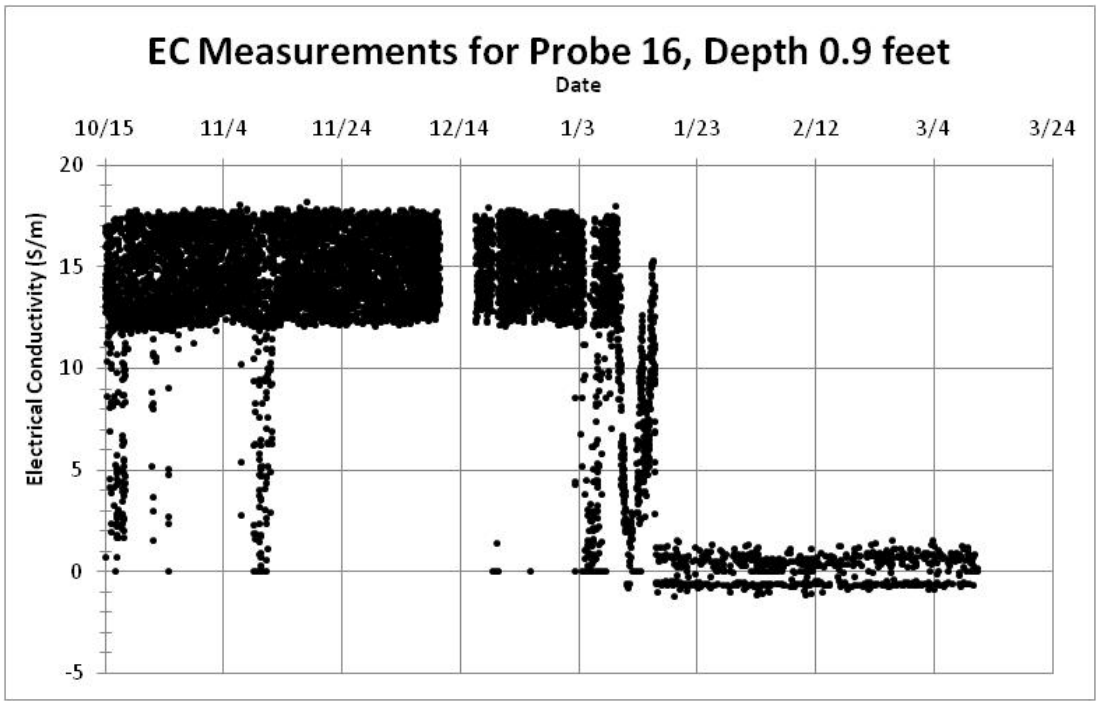

Figure 6.16: Electrical conductivity measurements for Probe 16

6.3: Troubleshooting

The main issue with the data from the TDR probes is the high electrical conductivity of the soil. High electrical conductivity of the soil causes attenuation of the signal which caused the end of the probe rods to not be seen in the waveform data. Without the end of the probes seen in the waveform data, the apparent probe length cannot be established. The moisture content of the soil is determined by the comparison of the apparent probe length compared to the actual probe length (L_a/L). The effects of the long cable lengths also exacerbate the problem of being able to identify the end of the probes in the high electrical conductivity soil.

6.3.1: Possible Solutions for Functioning Probes

Reedy and Scanlon (2002) correlated the moisture measurements to electrical conductivity since the waveform data also could not find the end of the probes. This method is not a likely solution for this study as there is too large of a scatter for filtering of the data.

A Fast Fourier Transform could be used on the waveform data to perform an analysis in the frequency domain (Jones and Or, 2004). Jones and Or (2004) found that the data could be recovered by using the Fast Fourier Transform in soils with electrical conductivity values five times greater than the upper limit in the time domain. The issue with using this method for this study is that Fast Fourier Transform method works better with very short probes lengths (on the order of two centimeters) while the probes for this study are 7.5 centimeters. Having shorter probes reduce the energy attenuation of the signal needed to perform analysis in the frequency domain.

Chen et al. (2007) discussed a method of using the TDR signal from the reflection at the surface of the soil instead of using the reflection from the end of the probe in soils

with a high electrical conductivity. This method could possibly be applied to this project. The model proposed by Chen et al. (2007) inverts the dielectric constant from the reflected signals at the soil surface. This model would require the TDR system currently in use to be recalibrated. Using this model could possibly be applicable for this project and could be further explored.

If the waveforms are not able to give values for the moisture content within the soil, the changes in the waveforms could be assessed to observe trends. Seeing a moisture front could be possible by observing changes to the waveforms. The amount of change or the exact moisture content could not be determined by conventional methods but a change in the waveform could indicate that the moisture front has reached the probes.

6.3.2: Possible Solutions for Non-Functioning Probes

The issue with the non-functioning probes is that they are not giving reasonable waveforms. A possible method for determining the problems is to inspect the probes near the surface by removing them. It is possible that fissures or voids are causing some of the probes to not work properly. If fissures or voids are an issue then it is possible that the clay could swell with an increase in moisture content and fill the fissures or voids. Inundating the volume of soil surrounding a probe would provide useful information regarding this issue. If the issue with the non-functioning probes can be determined then the probes could be reinstalled to try to minimize the problems.

CHAPTER 7: CONCLUSIONS

TDR probes were installed at a test wall in the highly expansive Taylor Clay in Manor, Texas. Monitoring of the moisture on site is important as the amount of lateral earth pressure exerted on the wall by the clay is related to the amount of moisture within the clay. Twenty TDR probes were installed in September and October 2010. The process of installing the probes and the initial results have been described in this thesis. The following conclusions can be drawn from this study.

- Currently, four of the 20 probes are recording waveforms that are functioning as expected. However, these waveforms cannot be analyzed by typical methods due to the waveforms not showing the reflection that indicates the end of the probe. The most likely reason for this is due to attenuation of the signal from the high electrical conductivity of the Taylor Clay. These waveforms are commonly seen in other studies with highly conductive soils (Campbell Scientific, Inc., 2010, Chen et al., 2007, Jones and Or, 2004, Reedy and Scanlon, 2002).
- The Campbell algorithm that finds the L_a/L values does not work with the waveforms received from the probes. The algorithm is unable to find the correct points on the waveforms due to noise within the waveforms and the waveforms not showing the reflection indicating the end of the probe.
- There is a large scatter of the electrical conductivity values for all the probes. Daily temperature effects are not apparent and the scatter is too large to reliably correlate to moisture content.

Problems with the TDR probes were exacerbated by the long cable lengths, short probe lengths, and the difficulty of installing the TDR probes in the soil. It is not possible to know if the probes were installed correctly at larger distances behind the wall. The Taylor Clay is filled with rocks and fossils that could have damaged the probes during installation. Also, it is not possible to know if the probes went through one of the many fissures that exist within the Taylor Clay.

7.1: Recommendations

More probes working properly would be needed to thoroughly monitor the moisture content behind the test wall. A possible method for determining the issues with the probes is to dig up some probes near the surface that are not working correctly and inspect them for possible issues. If fissures or voids caused by installation are causing some probes to not work properly then it is possible that when the moisture content increases, the clay could swell and fill the voids. Performing a test where the volume of soil around a probe near the surface is inundated with water could also provide useful information to this problem.

Even if the reason for the 16 probes not giving good waveforms is determined and fixed, they still could not be analyzed by the typical methods. Another method needs to be used to analyze the waveforms without the reflection point that indicates the end of the probe. Chen et al. (2007) developed a method which could be used for this study that does not need the reflection point that indicates the end of the probe.

Taking periodic physical measurements using a hand auger should be done to measure the moisture content of the soil. The physical measurements could supplement

the TDR measurements if the TDR data can be used. If the TDR measurements cannot be used then the physical measurements taken more often could provide the required moisture profile over time.

Appendix A

The following consists of the electrical conductivity figures for each of the 20 TDR probes.

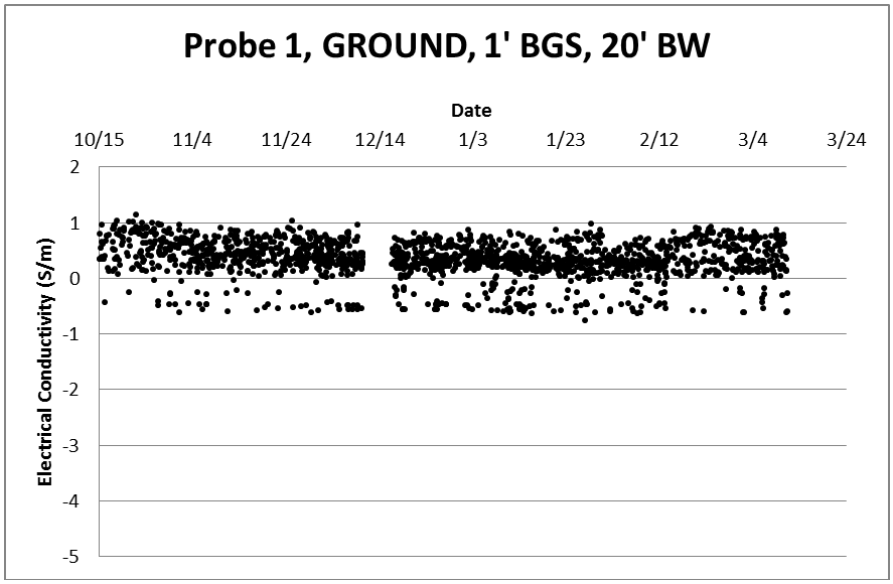

Figure A.1: Electrical conductivity for Probe 1 located 1 foot below the ground surface and 20 feet behind the wall

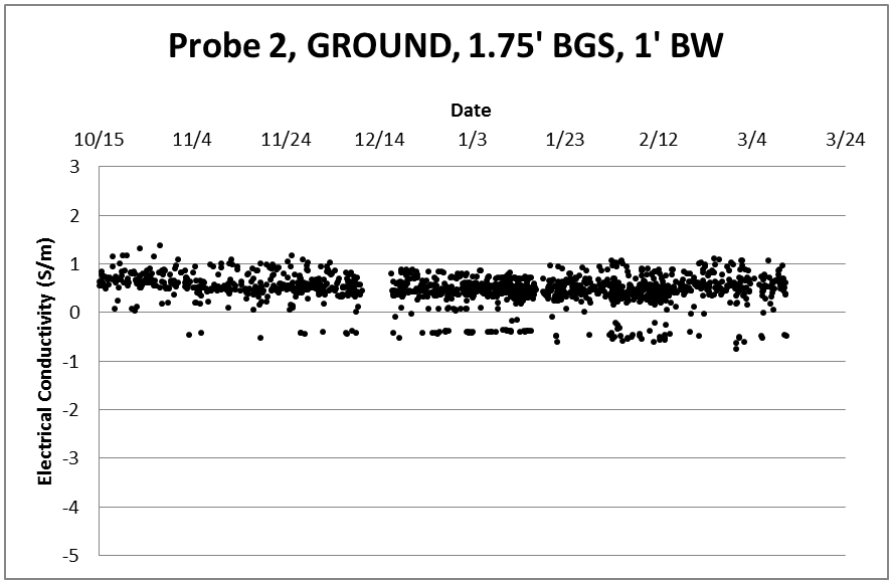

Figure A.2: Electrical conductivity for Probe 2 located 1.75 feet below the ground surface and 1 foot behind the wall

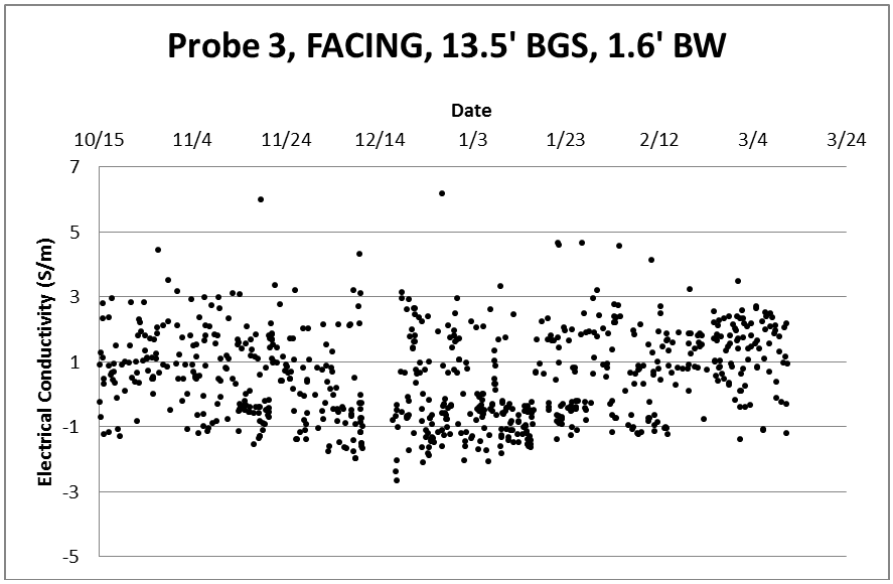

Figure A.3: Electrical conductivity for Probe 3 located 13.5 feet below the ground surface and 1.6 feet behind the wall

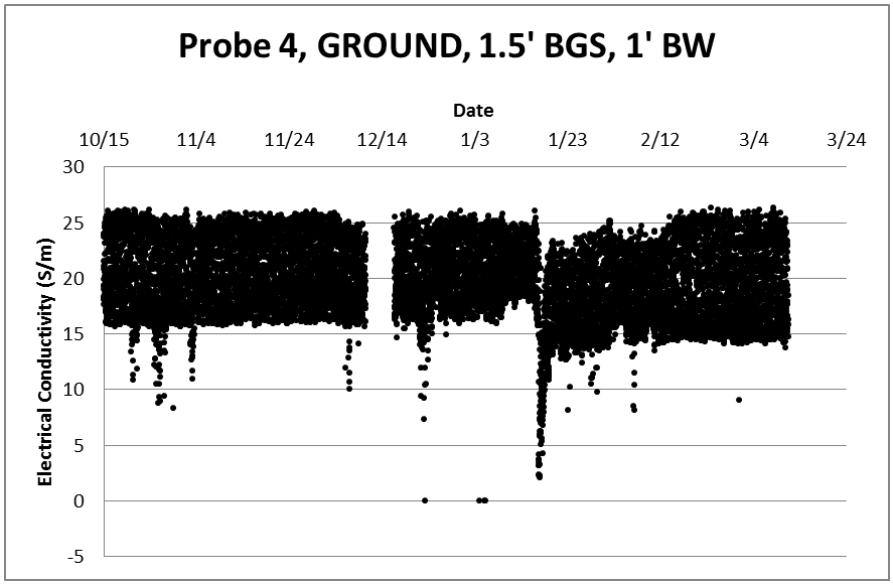

Figure A.4: Electrical conductivity for Probe 4 located 1.5 feet below the ground surface and 1 foot behind the wall

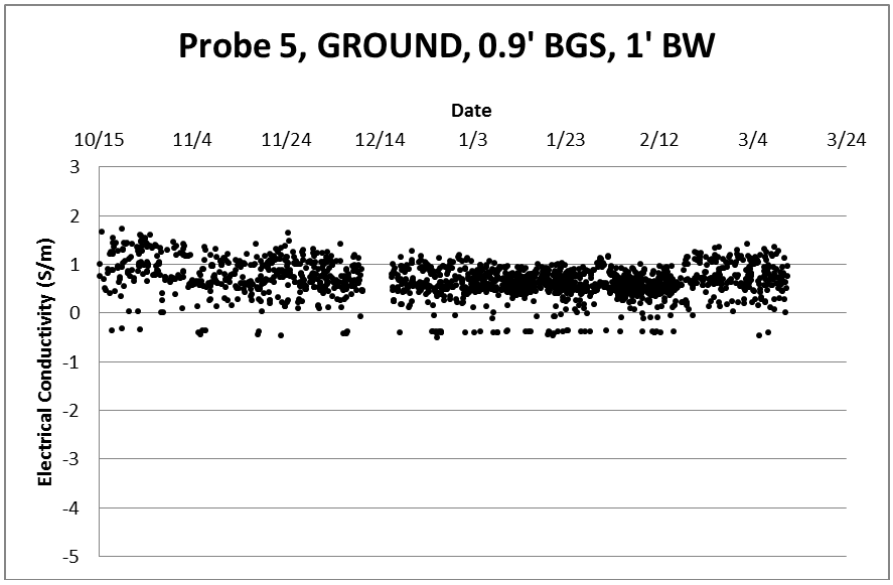

Figure A.5: Electrical conductivity for Probe 5 located 0.9 feet below the ground surface and 1 foot behind the wall

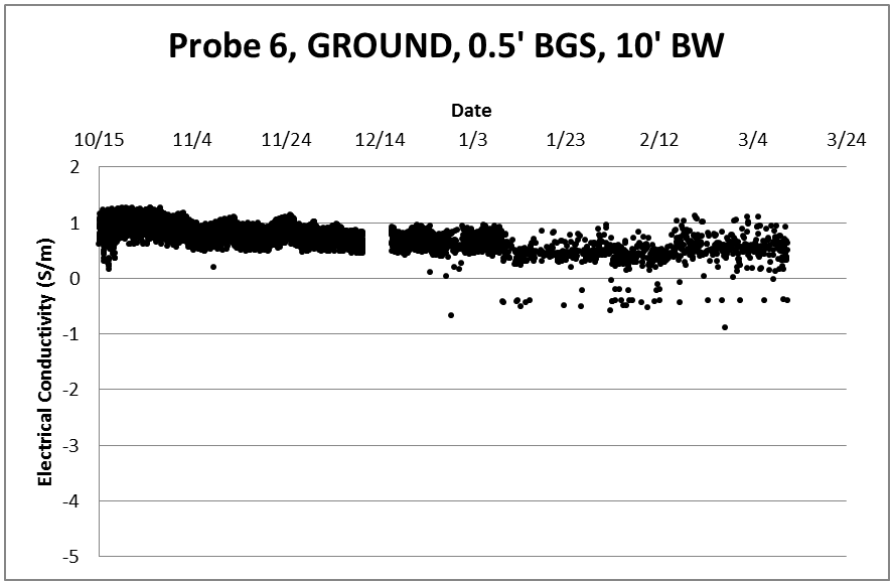

Figure A.6: Electrical conductivity for Probe 6 located 0.5 feet below the ground surface and 10 feet behind the wall

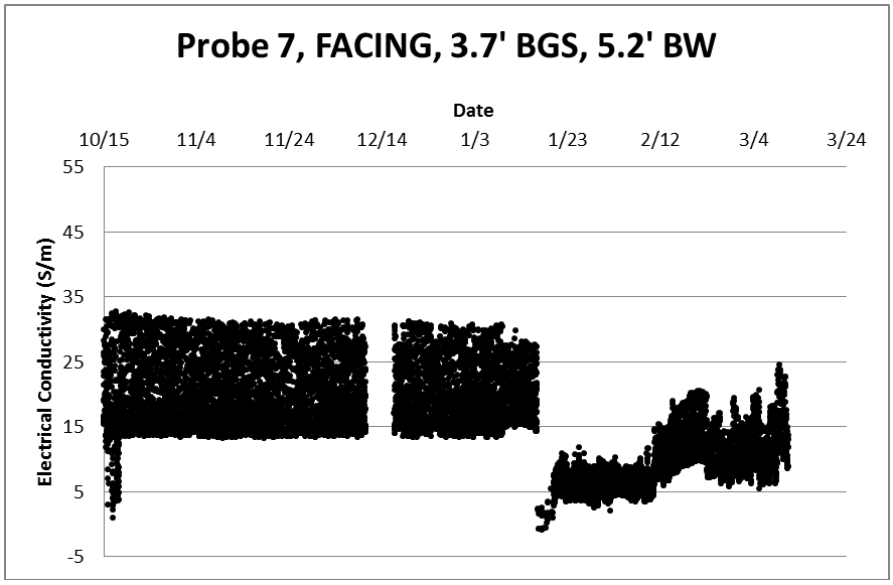

Figure A.7: Electrical conductivity for Probe 7 located 3.7 feet below the ground surface and 5.2 feet behind the wall

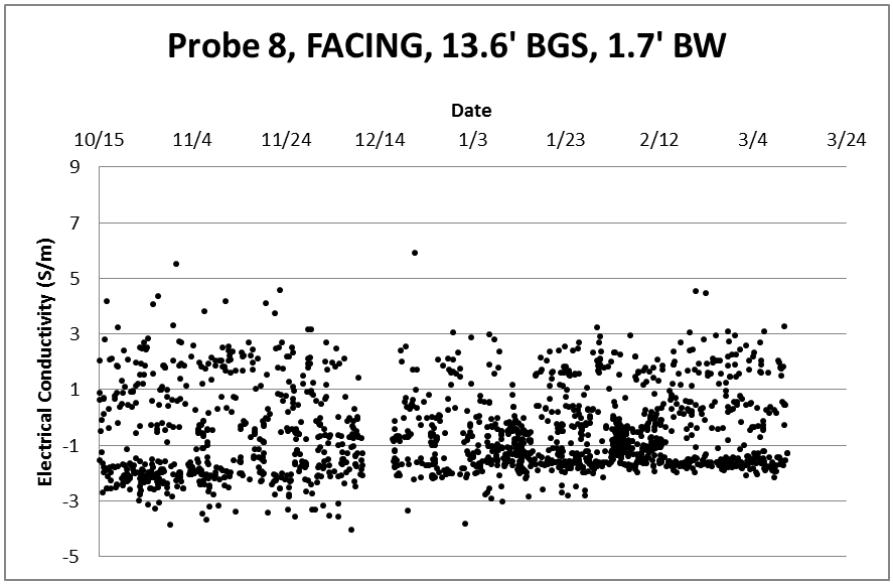

Figure A.8: Electrical conductivity for Probe 8 located 13.6 feet below the ground surface and 1.7 feet behind the wall

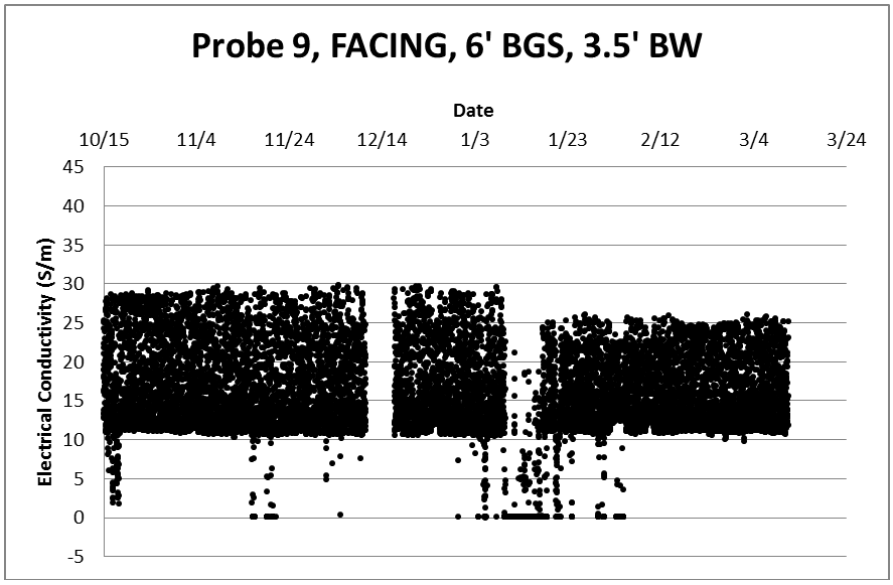

Figure A.9: Electrical conductivity for Probe 9 located 6 feet below the ground surface and 3.5 feet behind the wall

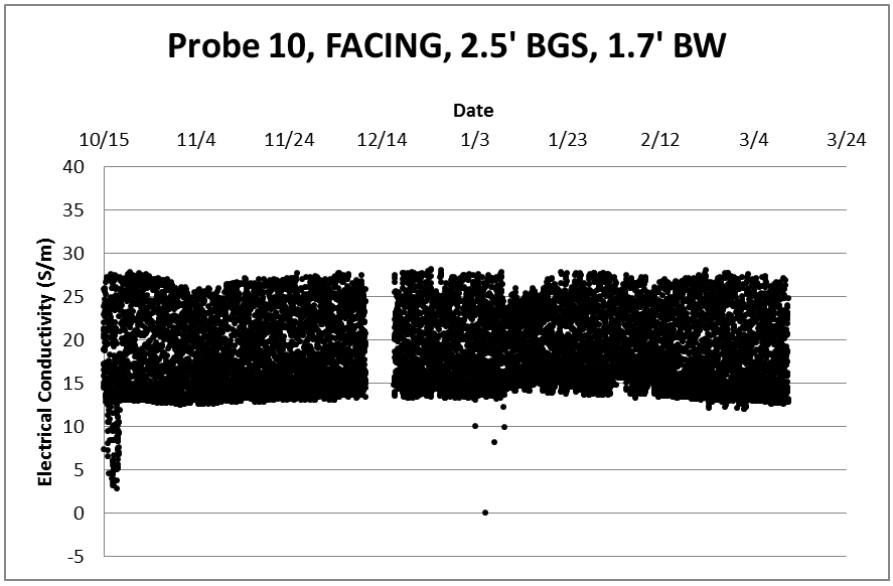

Figure A.10: Electrical conductivity for Probe 10 located 2.5 feet below the ground surface and 1.7 feet behind the wall

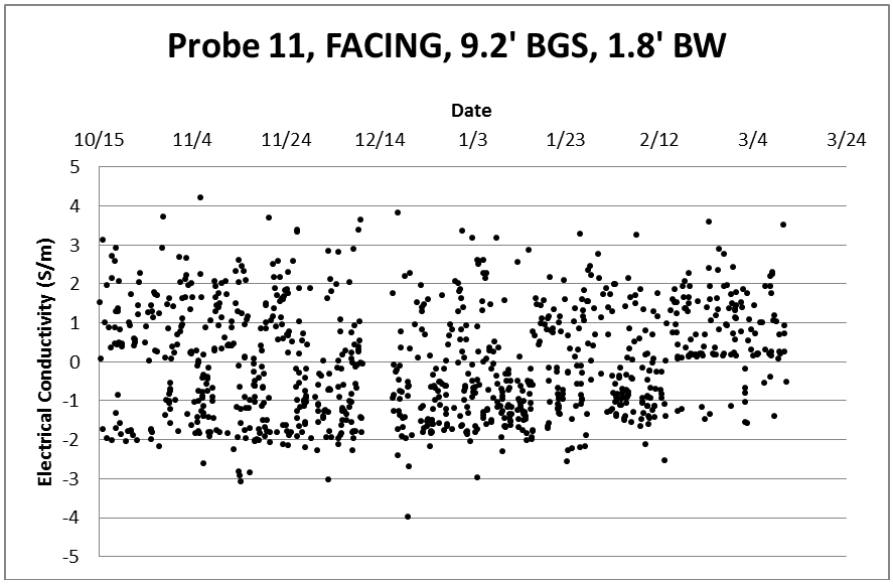

Figure A.11: Electrical conductivity for Probe 11 located 9.2 feet below the ground surface and 1.8 feet behind the wall

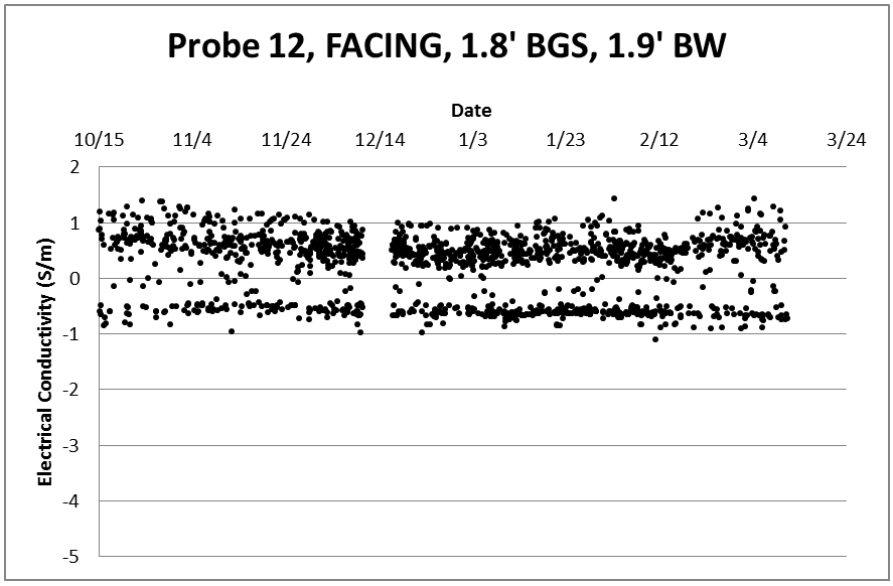

Figure A.12: Electrical conductivity for Probe 12 located 1.8 feet below the ground surface and 1.9 feet behind the wall

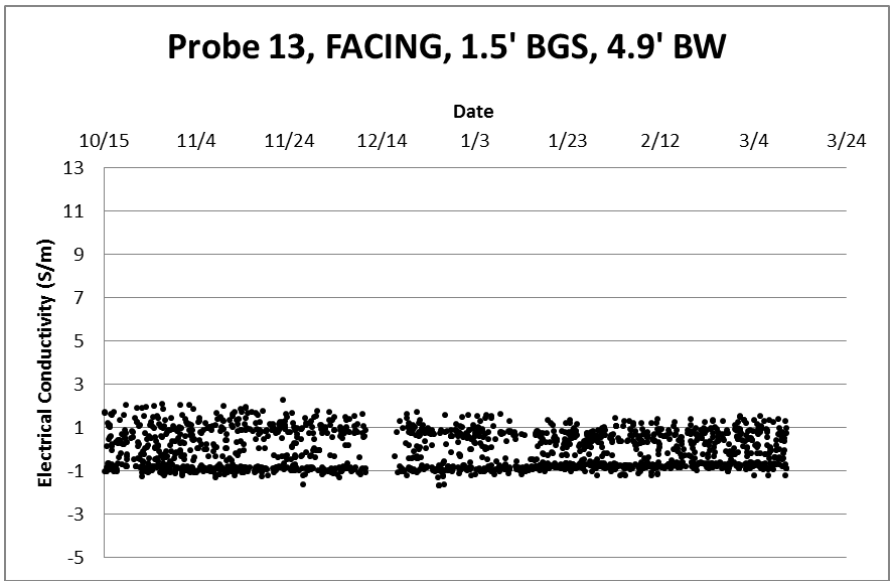

Figure A.13: Electrical conductivity for Probe 13 located 1.5 feet below the ground surface and 4.9 feet behind the wall

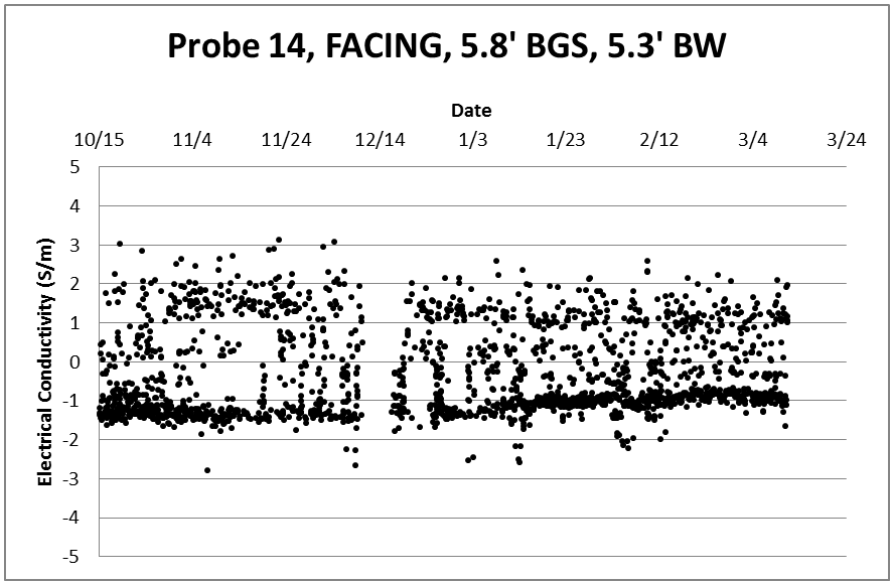

Figure A.14: Electrical conductivity for Probe 14 located 5.8 feet below the ground surface and 5.3 feet behind the wall

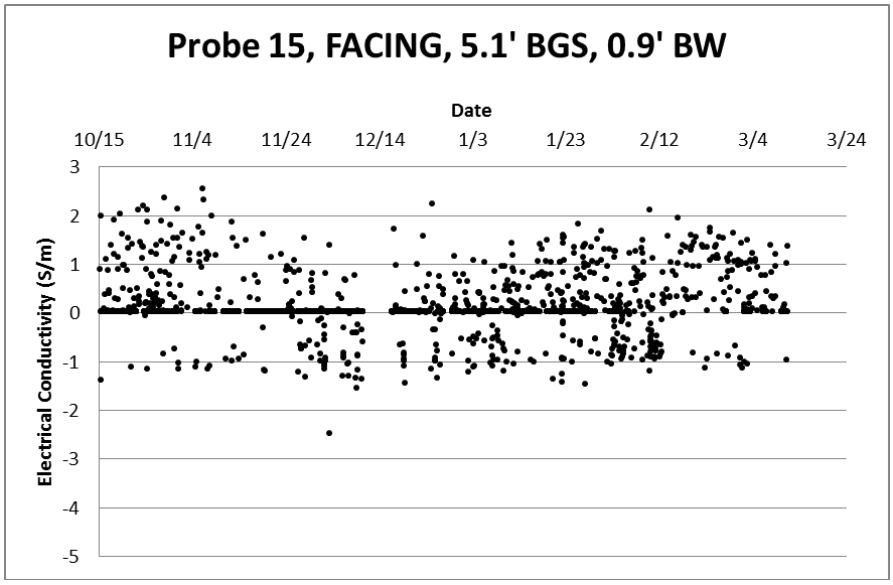

Figure A.15: Electrical conductivity for Probe 15 located 5.1 feet below the ground surface and 0.9 feet behind the wall

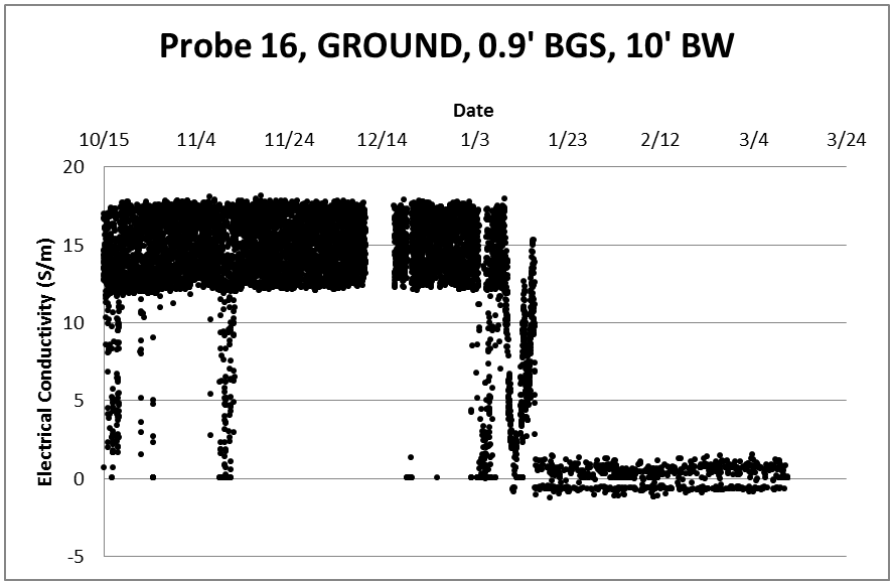

Figure A.16: Electrical conductivity for Probe 16 located 0.9 feet below the ground surface and 10 feet behind the wall

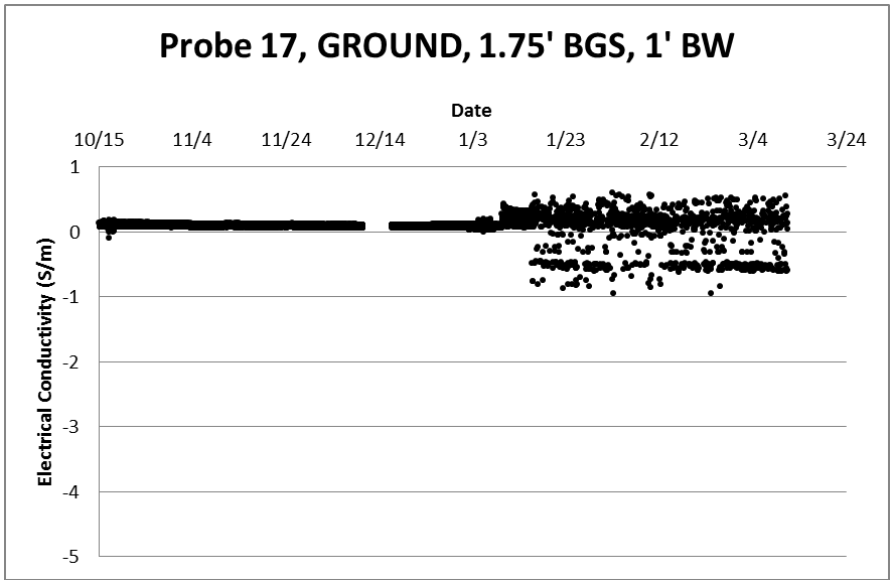

Figure A.17: Electrical conductivity for Probe 17 located 1.75 feet below the ground surface and 1 foot behind the wall

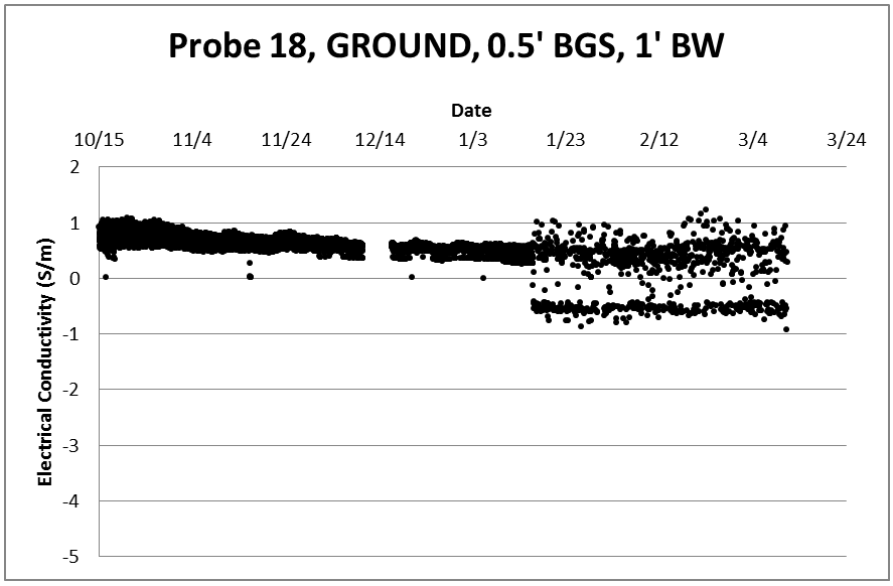

Figure A.18: Electrical conductivity for Probe 18 located 0.5 feet below the ground surface and 1 foot behind the wall

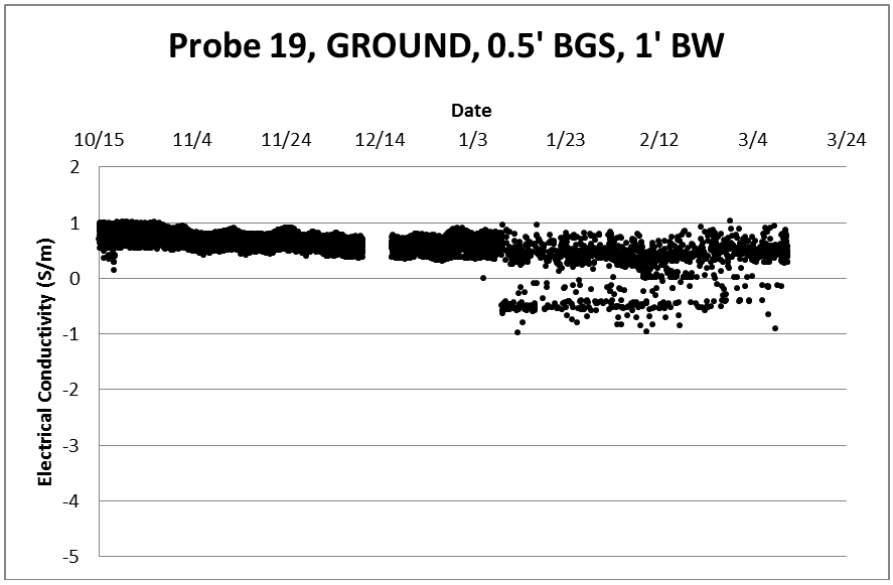

Figure A.19: Electrical conductivity for Probe 19 located 0.5 feet below the ground surface and 1 foot behind the wall

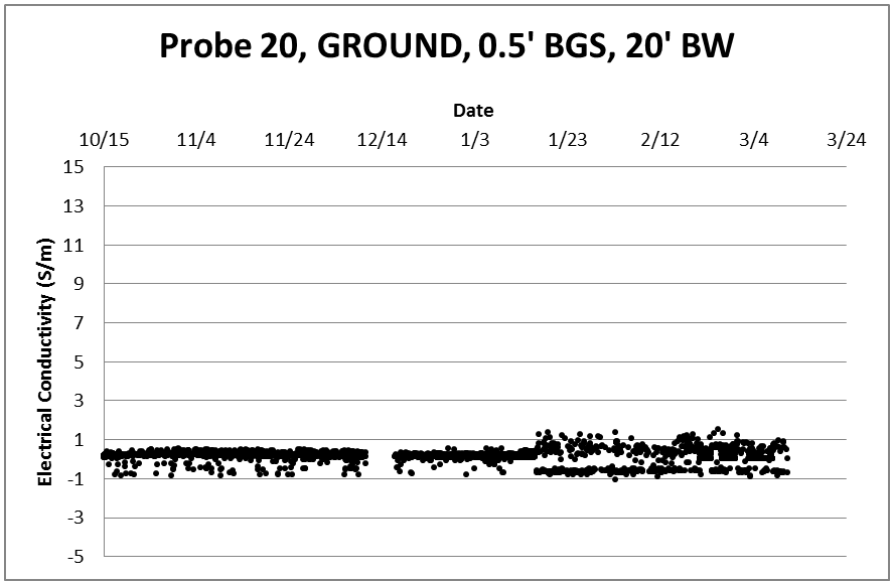

Figure A.20: Electrical conductivity for Probe 20 located 0.5 feet below the ground surface and 20 feet behind the wall

Appendix B

The following consists of the L_a/L versus time figures for each of the 20 TDR probes.

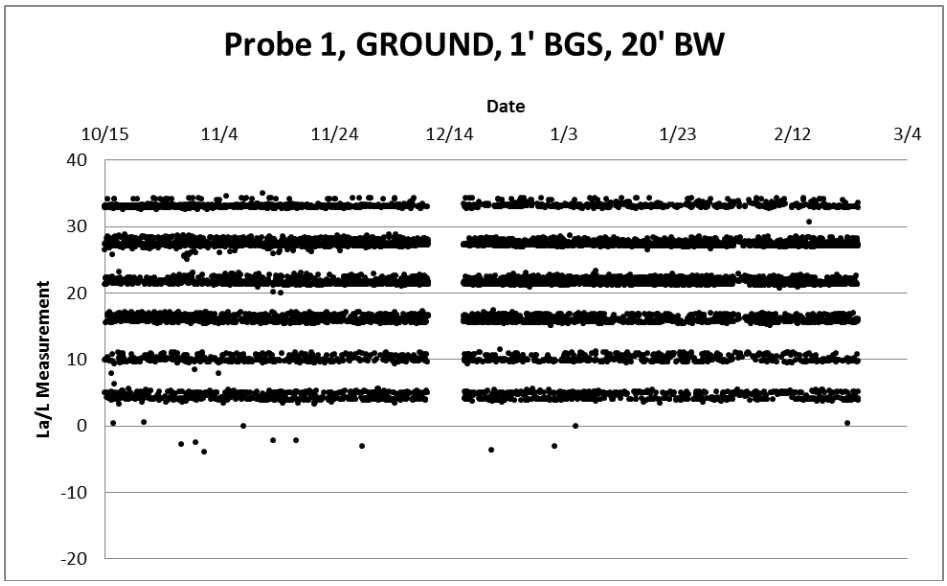

Figure B.1: L_a/L values for Probe 1 located 1 foot below the ground surface and 20 feet behind the wall

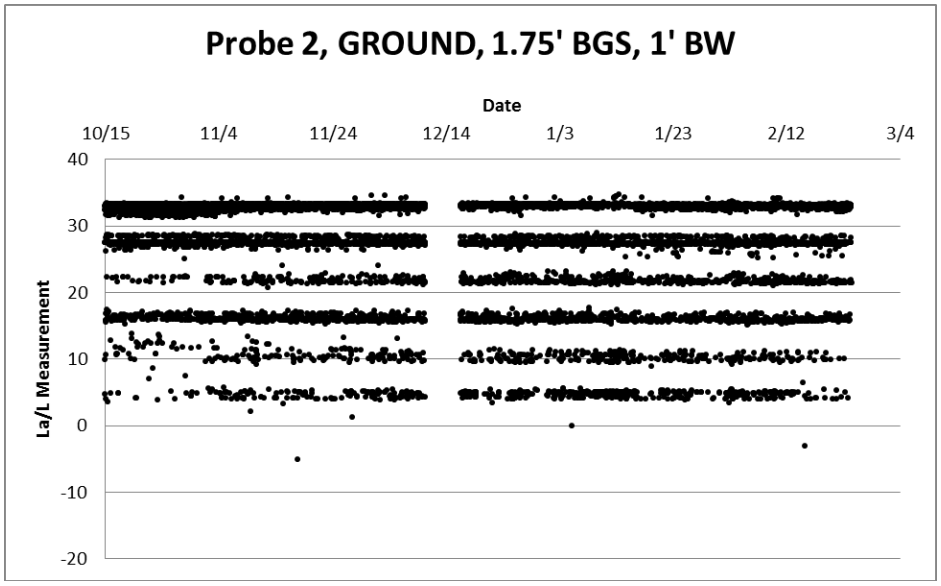

Figure B.2: L_a/L values for Probe 2 located 1.75 feet below the ground surface and 1 foot behind the wall

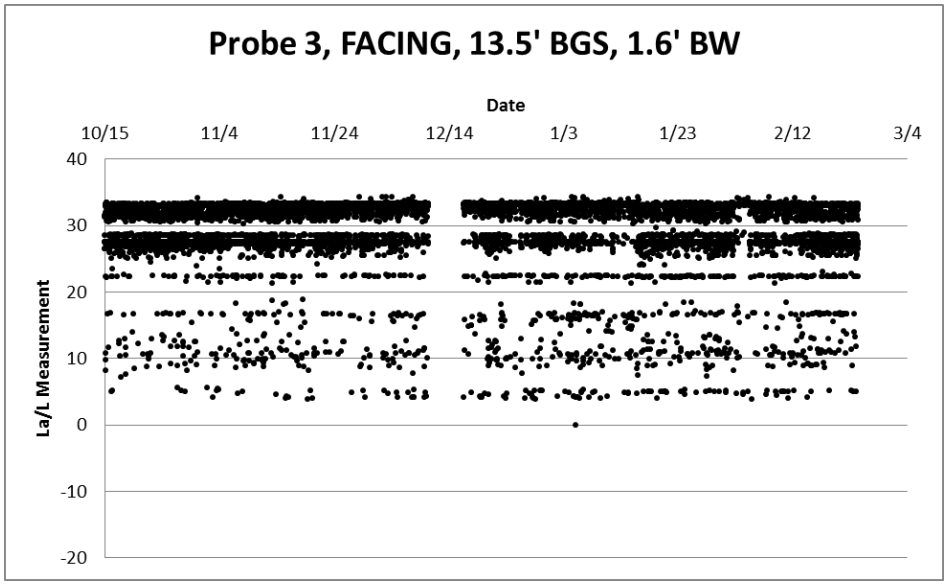

Figure B.3: L_a/L values for Probe 3 located 13.5 feet below the ground surface and 1.6 feet behind the wall

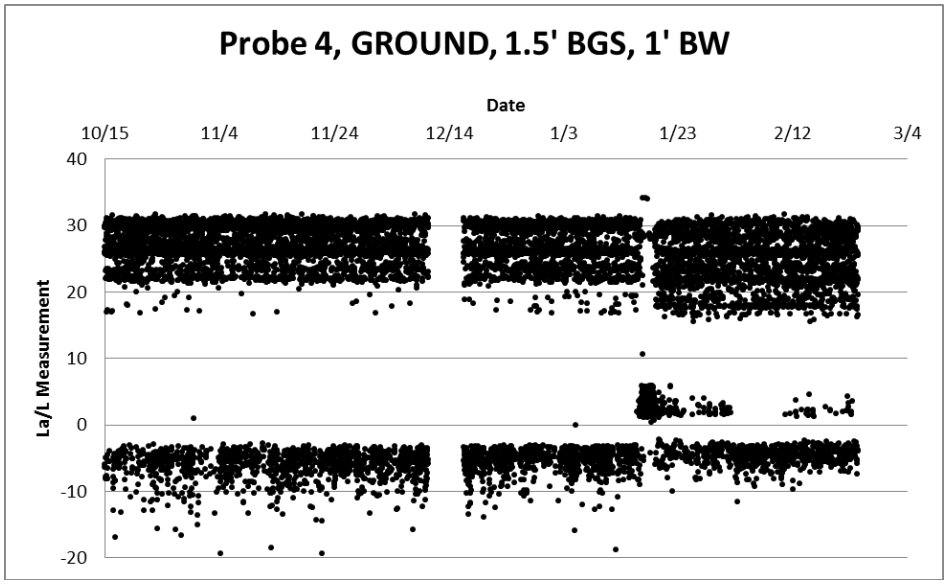

Figure B.4: L_a/L values for Probe 4 located 1.5 feet below the ground surface and 1 foot behind the wall

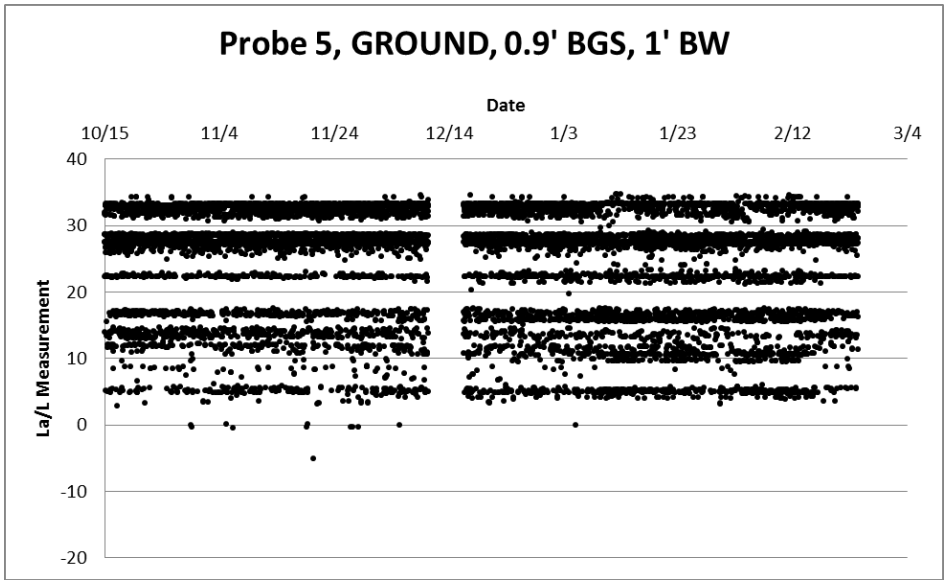

Figure B.5: L_a/L values for Probe 5 located 0.9 feet below the ground surface and 1 foot behind the wall

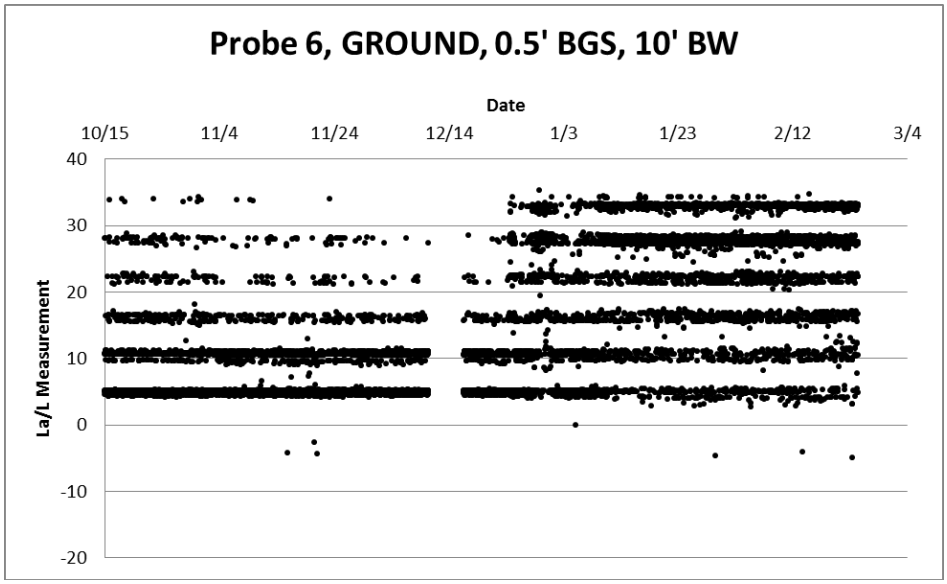

Figure B.6: L_a/L values for Probe 6 located 0.5 feet below the ground surface and 10 feet behind the wall

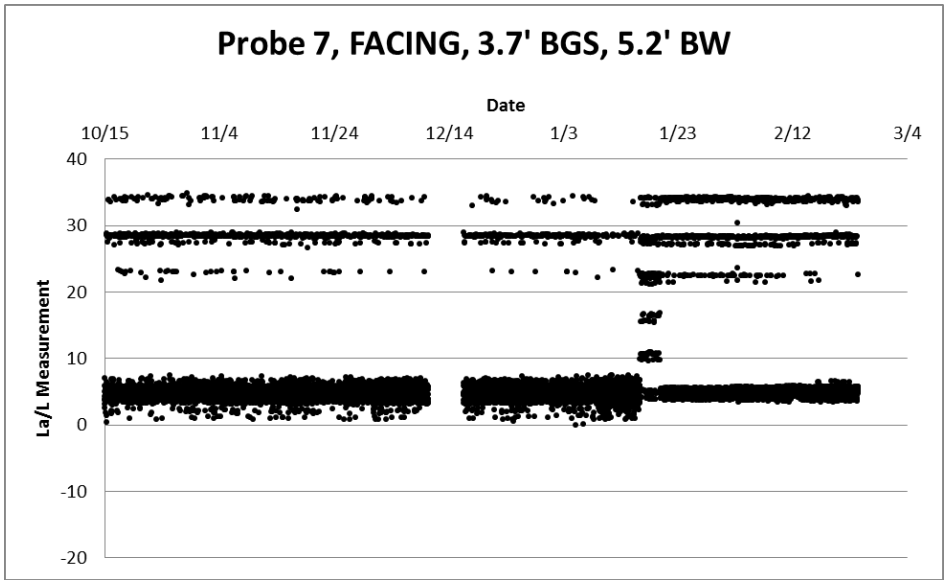

Figure B.7: L_a/L values for Probe 7 located 3.7 feet below the ground surface and 5.2 feet behind the wall

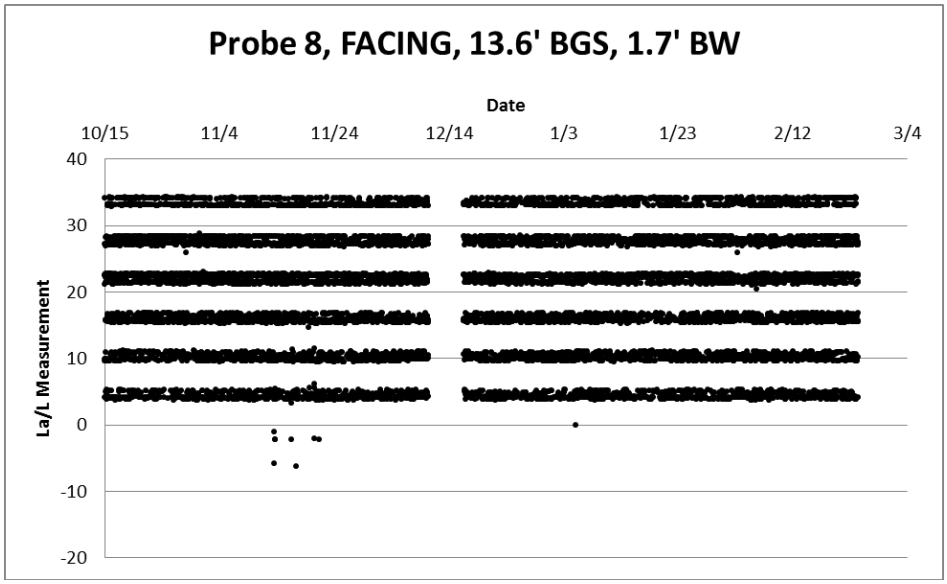

Figure B.8: L_a/L values for Probe 8 located 13.6 feet below the ground surface and 1.7 feet behind the wall

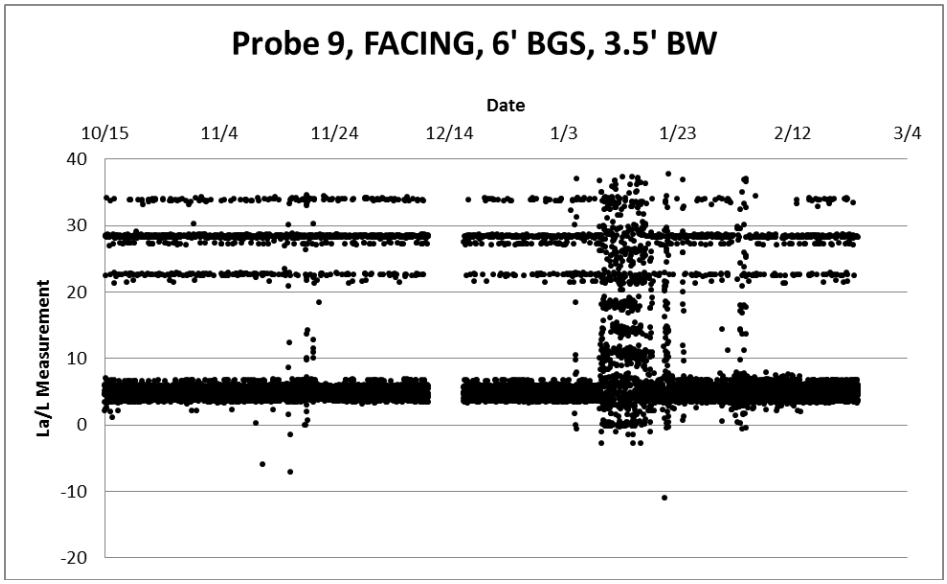

Figure B.9: L_a/L values for Probe 9 located 6 feet below the ground surface and 3.5 feet behind the wall

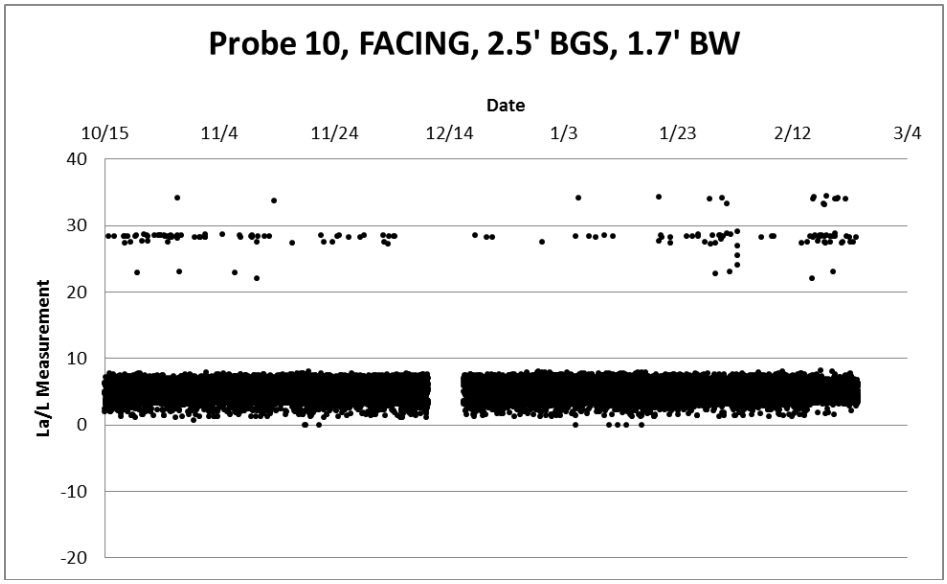

Figure B.10: L_a/L values for Probe 10 located 2.5 feet below the ground surface and 1.7 feet behind the wall

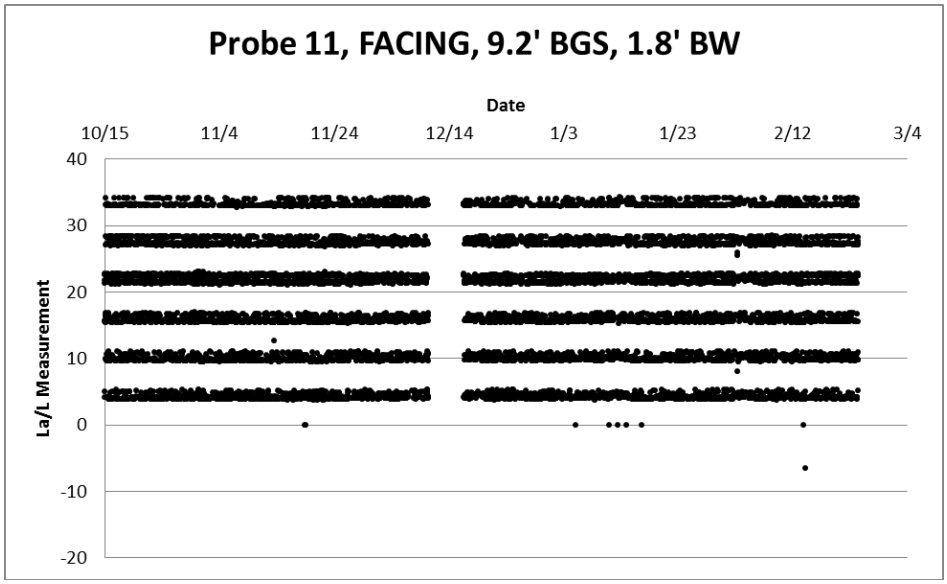

Figure B.11: L_a/L values for Probe 11 located 9.2 feet below the ground surface and 1.8 feet behind the wall

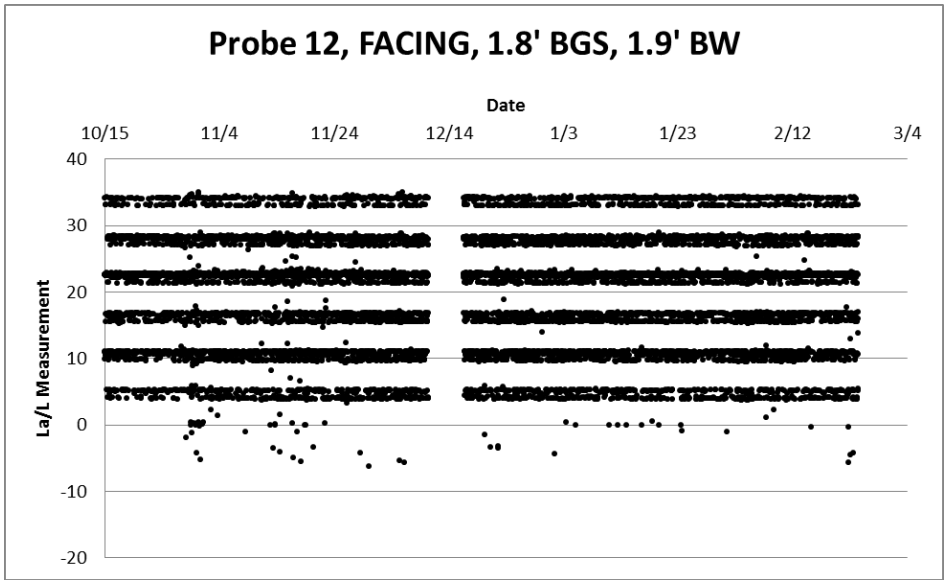

Figure B.12: L_a/L values for Probe 12 located 1.8 feet below the ground surface and 1.9 feet behind the wall

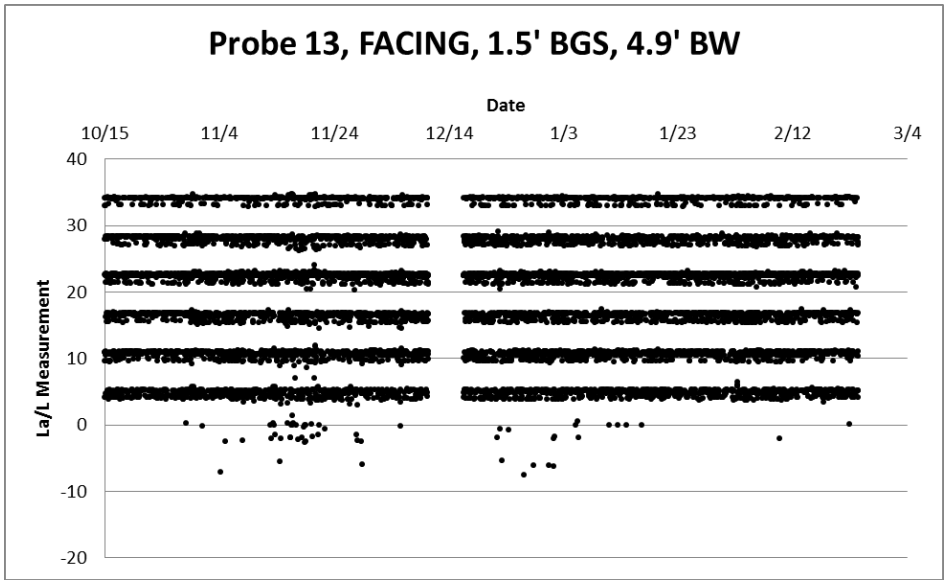

Figure B.13: L_a/L values for Probe 13 located 1.5 feet below the ground surface and 4.9 feet behind the wall

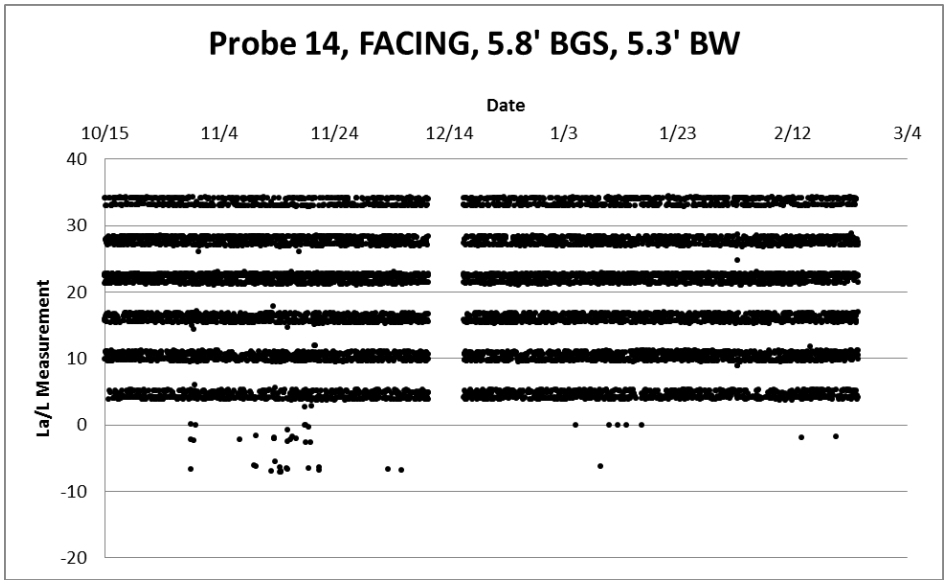

Figure B.14: L_a/L values for Probe 14 located 5.8 feet below the ground surface and 5.3 feet behind the wall

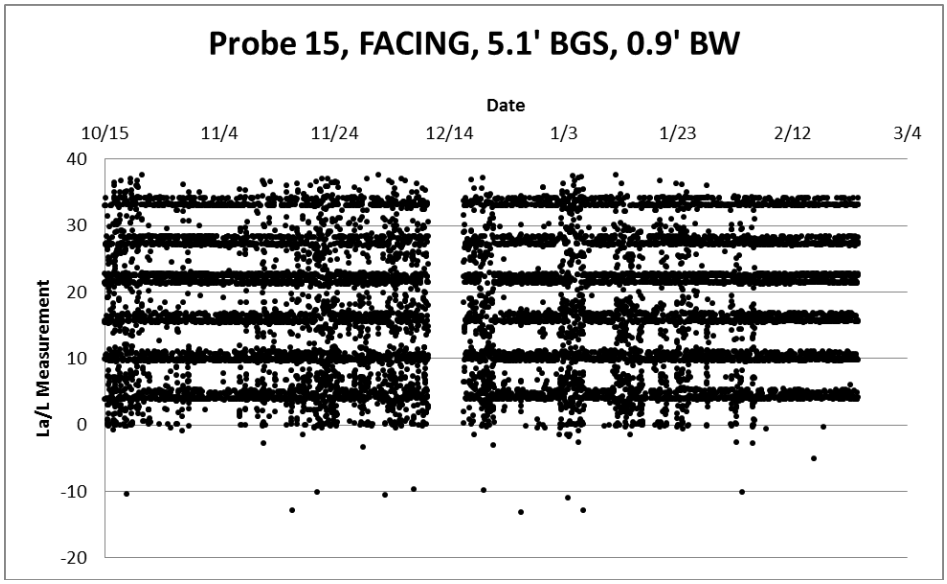

Figure B.15: L_a/L values for Probe 15 located 5.1 feet below the ground surface and 0.9 feet behind the wall

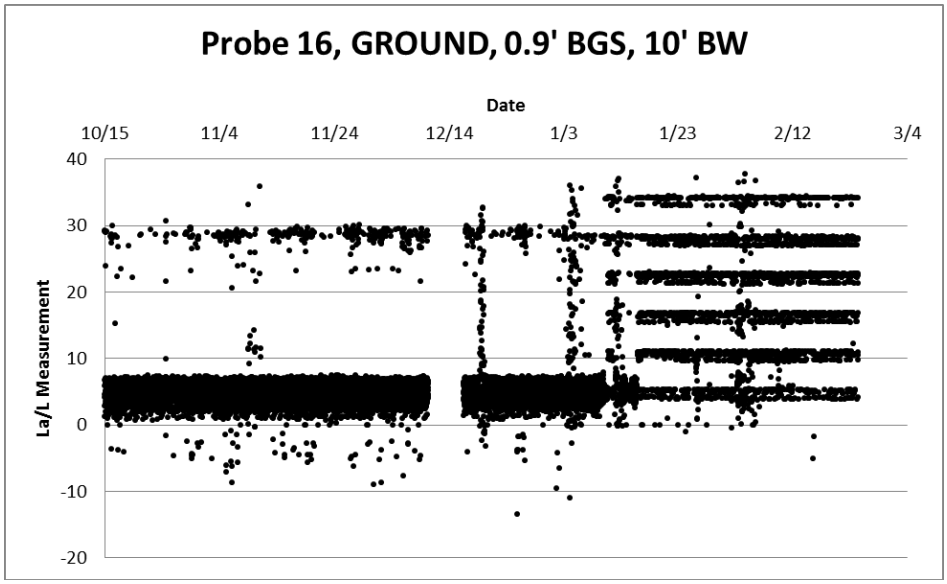

Figure B.16: L_a/L values for Probe 16 located 0.9 feet below the ground surface and 10 feet behind the wall

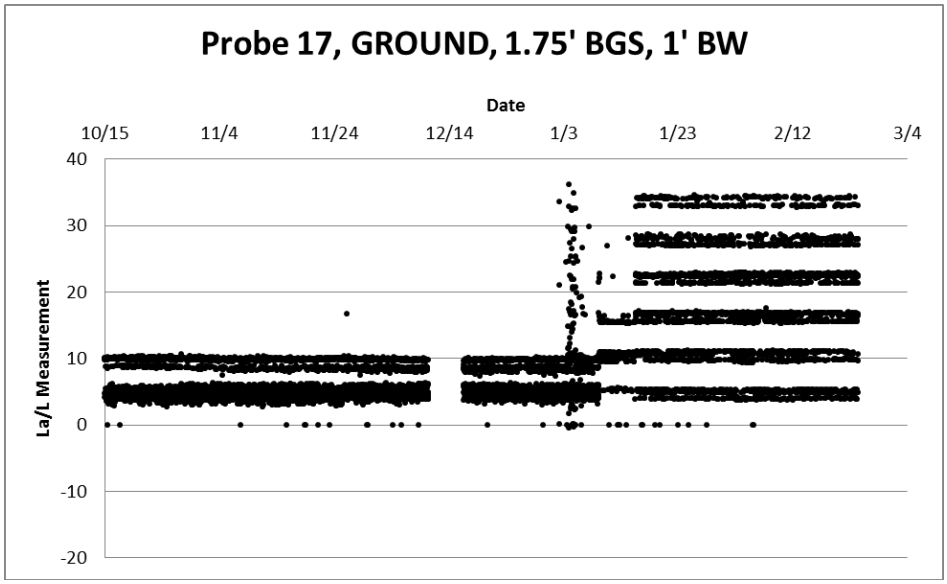

Figure B.17: L_a/L values for Probe 17 located 1.75 feet below the ground surface and 1 foot behind the wall

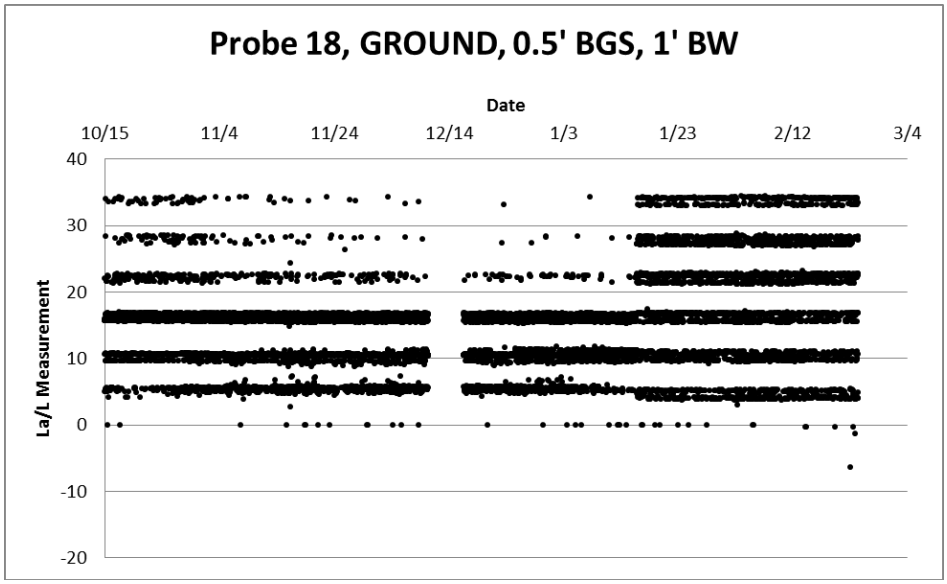

Figure B.18: L_a/L values for Probe 18 located 0.5 feet below the ground surface and 1 foot behind the wall

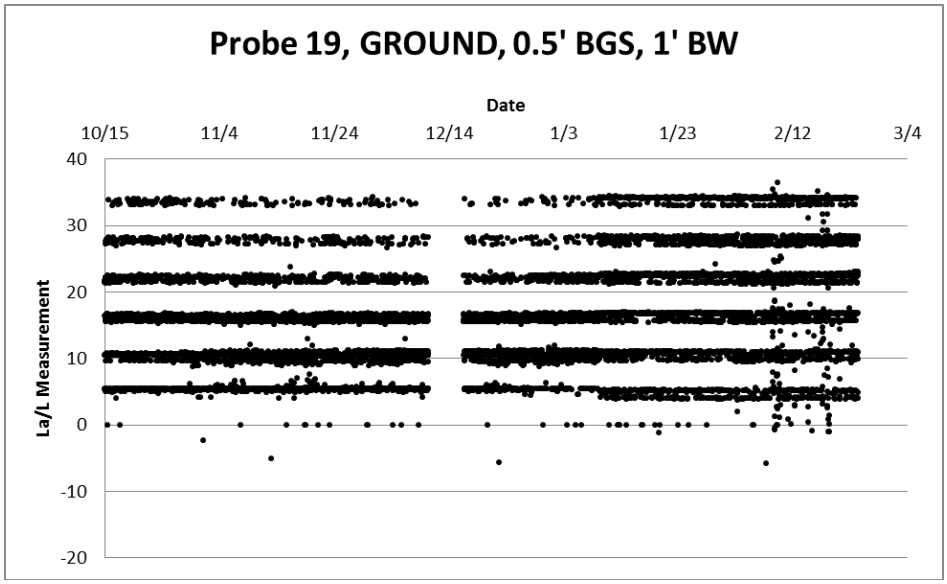

Figure B.19: L_a/L values for Probe 19 located 0.5 feet below the ground surface and 1 foot behind the wall

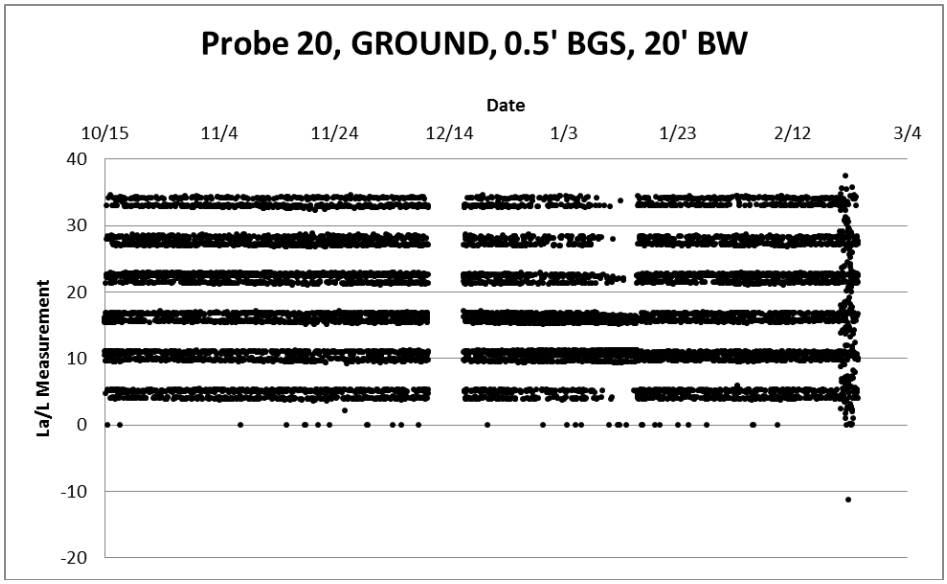

Figure B.20: L_a/L values for Probe 20 located 0.5 feet below the ground surface and 20 feet behind the wall

References

Antle, Chad L. Soil Moisture Determination by Frequency and Time Domain Techniques. Master's Thesis, Ohio University, 1997

Brown, A. C., Ellis, T., Dellinger, G., El-Mohtar, C., Zornberg, J., & Robert, G. B. (2011). Long-term monitoring of a drilled shaft retaining wall in expansive clay: Behavior before and during excavation. Geo-Frontiers 2011: Advances in Geotechnical Engineering , 3516-3525.

Brown, J. "TDR Probe Rod Deflection" Email to Andy Brown. August 2011

Campbell Scientific, Inc. (2010). TDR100 Instruction Manual.

Campbell Scientific, Inc. Tech Support (2010). Personal Communication. Campbell Scientific, Inc., Logan, Utah.

Chen, R., Drnevich, V. P., Yu, X., Nowack, R. L., & Chen, Y. (2007). Time Domain Reflectometry Surface Reflections for Dielectric Constant in Highly Conductive Soils. Journal of Geotechnical and Geoenvironmentaal Engineering , 133, 1597-1608.

Dean, T. J., Bell, J. P., & Baty, A. J. (1987). Soil Moisture Measurement by an Improved Capacitance Technique, Part 1. Sensor Design and Performance. Journal of Hydrology , 93, 67-78.

Foundation Engineering Handbook (1991), Second Edition, Edited by H-Y. Fang, Van Nostrand Reinhold, New York.

Ellis, Trent. A Subsurface Investigation in Taylor Clay. Master's Thesis, The University of Texas at Austin, 2011

Gaskin, G. J., & Miller, J. D. (1996). Measurement of Soil Water Content Using a Simplified Impedance Measuring Technique. Journal of Agricultural Engineering Research , 63, 153-160.

Giese, K., & Tiemann, R. (1975). Determination of the complex permittivity from thin-sample time domain reflectometry, Improved analysis of the step response waveform. Advances in Molecular Relaction Processes , 7 (1), 45-59.

Jarell, Glenn, 2010, Personal Communication. Campbell Scientific, Inc., Logan, Utah.

Jarell, G., Ritter, J. “GJ & Jason/csi review c/o Andy Brown interpreting erratic TDR100 La/L & EC measurement Ref: UT Manor Wall” Email to Andy Brown. April 2011

Jones, D. J., & Holtz, W. (1973). Expansive Soils - The Hidden Disaster. Civil Engineering , 43, 49-51.

Jones, S. B., & Or, D. (2004). Frequency Domain Analysis for Extending Time Domain Reflectometry Water Content Measurement in Highly Saline Soils. Soil Science Society of America Journal , 68, 1568-1577.

Kuhn, Jeffrey. Effect of Cracking on the Hydraulic Properties of Unsaturated Highly Plastic Clays. Master’s Thesis, The University of Texas at Austin, 2005

Moret-Fernandez, D., Lera, F., Arrue, J. L., & Lopez, M. V. (2009). Measurement of Soil Bulk Electrical Conductivity Using Partially Coated TDR Probes. Valdose Zone Journal , 8 (3), 594-600.

Patterson, D. E., & Smith, M. W. (1985). Unfrozen water content in saline soils: results using time-domain reflectometry. Canadian Geotechnical Journal , 22, 95-101.

Reedy, R. C., and Scanlon, B. R., 2002, Long-term water balance monitoring of engineered covers for waste containment, in2001 International Containment and Remediation Technology Conference, Orlando, Florida, Institute for International Cooperative Environmental Research, Florida State University, Paper ID. No. 073, http://www.iicer.fsu.edu, 3 p

Reedy, Robert, 2010, Personal Communication. Bureau of Economic Geology, Austin, Texas.

Roth, K., Schulin, R., Fluhler, H., & Attinger, W. (1990). Calibration of Time Domain Reflectometry for Water Content Measurement Using a Composite Dielectric Approach. Water Resources Research , 26 (10), 2267-2273.

Seyfriend, M. S., & Murdock, M. D. (2004). Measurement of Soil Water Content with a 50-MHz Soil Dielectric Sensor. Soil Science Society of America Journal , 68, 394-403.

Siddiqui, S. I., Drnevich, V. P., & Deschamps, R. J. (2000). Time Domain Reflectometry Development for Use in Geotechnical Engineering. Geotechnical Testing Journal , 23, 9-20.

Topp, G. C., Davis, J. L., & Annan, A. P. (1980). Electromagnetic Determination of Soil Water Content Measurements in Coaxial Transmission Lines. Water Resources Research, 16 (3), 574-582.